[AMERICAN JOURNAL OF SCIENCE, VOL. 283, FEBRUARY, 1983, P. 97-134]

American Journal of Science

FEBRUARY 1983

KYANITE–STAUROLITE METAMORPHISM IN SULFIDIC SCHISTS OF THE ANAKEESTA FORMATION, GREAT SMOKY MOUNTAINS, NORTH CAROLINA

D. W. MOHR* and R. C. NEWTON**

ABSTRACT. *A sequence of dark schists with variable pyrrhotite and graphite contents is exposed in the northern terminus of the Murphy Syncline. These schists, correlated with the Anakeesta Formation of probable late Precambrian age, show a Barrovian metamorphic gradation from the garnet zone through staurolite and kyanite isograds to middle kyanite grade in the Fontana Lake area, N.C. Many aspects of the prograde mineral development were controlled by variable sulfur fugacity and attendant Fe depletion of the silicates. The most sulfur-rich rocks, termed "black schists," show very Mn-rich garnets, Mg-rich, K-poor biotite, and rutile, with development of kyanite but not staurolite at high grades. Sulfur-poor rocks, termed "gray schists," have Fe-richer garnets and biotite, and ilmenite, and develop staurolite but not kyanite at higher grades. A few intermediate rocks have both ilmenite and rutile and develop both kyanite and staurolite. The kyanite and staurolite isograds are thus compositionally restricted. The latter isograd is well-defined and close to, but at slightly lower grade than, the kyanite isograd, which is more diffuse. The isogradic reactions are of chlorite and white mica to staurolite or kyanite and biotite. Garnet is probably a participant in the staurolite-forming reaction, which is nearly univariant. The kyanite-forming reaction may be of higher variance, because of lack of participation of garnet, which is present in the black schists only through Mn-stabilization.*

Mineralogic geothermometry-geobarometry fix the conditions of the staurolite-and-kyanite metamorphism at 580°C ± 35°C and 6.6 ± 0.9 kb. The partial pressure of H_2O was high, probably greater than 85 percent of total pressure. CO_2 pressure was substantial; the partial pressures of sulfur-bearing vapor species was low. P_{O_2} was controlled to low values by ubiquitous graphite. The observed pyrrhotite composition of $Fe_{0.91 \pm 0.01}S$ may be representative of the metamorphism and has apparently not changed by back-reaction, although supergene pyrite or marcasite has replaced much of it.

A number of mineralogic peculiarities of the metamorphism may possibly be explained directly or indirectly by high sulfur contents of the black schists, including Na-rich high-grade rims of plagioclase porphyro-

* Department of Geology, Texas A and M University, College Station, Texas 77843
** Department of the Geophysical Sciences, University of Chicago, Chicago, Illinois 60637

blasts (normal zoning), low alkali contents of biotite, Mn-rich rims of high-grade garnets, and prograde appearance of paragonite as a discrete phase coexisting with plagioclase in the kyanite zone ("paragonite–plagioclase isograd").

The sulfur and carbon contents of unweathered schists are highly correlative and probably of sedimentary and diagenetic origin. Subsequent metamorphism converted pyrite to pyrrhotite with attendant Fe-depletion of silicates. No significant transport of sulfur occurred during the metamorphism. Metamorphic reactions which gave rise to the characteristic observed mineralogic features were greatly influenced by the small amount of iron available to the silicate phases as a result of the sulfur-rich bulk compositions.

INTRODUCTION

Previous work on sulfide–silicate metamorphism.—Metamorphism of pelitic and psammitic rocks containing abundant iron sulfide, with or without graphite, has been described from several localities in the past decade. The important controls that the sulfides can exercise on the major mineralogy are just beginning to be understood; it has only recently been recognized that the ubiquitous "opaques" in metasediments, which have been traditionally disregarded unless they are abundant enough to constitute ore deposits, can have subtle but profound influence on the career of progressive metamorphism. Earlier writers (for example, Marmo and Mikkola, 1951; Vokes, 1969) were concerned mainly with the mineralogy and metamorphic textures of sulfides and paid scant attention to the associated silicates.

The common phenomenon of iron depletion of the ferromagnesian silicates in middle and high grade metamorphic sulfidic rocks, which may have very important consequences in the index-mineral sequence, was not seriously studied before 1977, although certain aspects of the process were noted briefly by several workers. Prograde, nearly isogradic appearance of pyrrhotite replacing pyrite has been noted briefly several times (Guidotti, 1970; Bachinski, 1976; French, 1968; Carpenter, 1974), and some authors have suggested that such a reaction can accomplish iron depletion of the coexisting silicates. For example, in a study of contact metamorphism at Notre Dame Bay, Newfoundland, Bachinski (1976) suggested the general reaction:

$$\text{pyrite} + \text{Fe–silicates} = \text{pyrrhotite} + \text{Fe-poorer silicates} \qquad \text{(A)}$$

to account for the very magnesian compositions of ferromagnesian silicates in sulfide-bearing, mafic volcanic rocks at high metamorphic grade. Salotti (1969) invoked a similar mechanism to explain progressive iron depletion in silicates during prograde metamorphism of ore and gangue minerals of the sulfide ore bodies at Ducktown, Tenn. Thompson (1972), interpreting the mineralogic data of Guidotti (1970) for the high grade sulfidic schists of the Oquossoc area, northern Maine, suggested, as an isogradic reaction for the appearance of pyrrhotite:

$$\text{pyrite} + \text{biotite} + \text{sillimanite} + \text{graphite} = \text{pyrrhotite} + \text{muscovite} + \text{quartz} + CO_2, \qquad \text{(B)}$$

which is essentially an iron-depletion reaction, ferromagnesian mica giving way to white mica. However, the regional appearance of pyrrhotite in schists of the Great Smoky Mountains area occurs in the chlorite zone and is not obviously associated with any isogradic event in the silicates (Carpenter, 1974).

Several authors have noted, almost incidentally, that the partitioning of iron from silicates into sulfides at higher grades gives rise to some unusual parageneses. Clark (1969) reported extremely Mg-rich cordierite in sulfidic schists from Portugal. Guidotti, Cheney, and Conatore (1975a) described the rare assemblage cordierite–chlorite in the sillimanite zone of the sulfide-rich Small's Falls Formation, northwestern Maine. Here chlorite is especially refractory because of its high Mg/(Mg + Fe) ratio, which, in turn, results from Fe loss to sulfides. Guidotti, Cheney, and Conatore (1975b) gave analyses of biotites with unusual compositions from the staurolite zone in the Small's Falls Formation. The alkali contents average about 1.55 atoms per 22 oxygens, compared to the theoretical 2.0. These biotites are also very Mg-rich and TiO_2-poor. Guidotti (1974) correlated occasional high Mn contents of garnets with local concentrations of sulfides in high grade schists of the Rangeley Quadrangle, Maine. Mn-rich garnets at high grade were also noted by Tracy (1978) in sulfide- and graphite-bearing schists, west-central Massachusetts. Itaya and Banno (1980) found garnets with up to 5 wt percent MnO in sulfidic, carbonaceous schists of the Sanbagawa belt, central Shikoku. At low grades, sphene is the only Ti-bearing accessory, but ilmenite and rutile appear at higher grades. Guidotti, Cheney, and Conatore (1975b) noted that rutile occurs in the very pyrrhotite-rich sections of the Small's Falls rocks and ilmenite in the others. None of the above authors analyzed the unusual mineralogic features from the standpoint of sulfur activity.

A new and more analytical direction was taken by Robinson and Tracy (1977). They recognized the controlling influence of the several percent of pyrite, pyrrhotite, and graphite over the major mineral parageneses in the sulfidic Paxton Schist of central Massachusetts and wrote sulfides as participants in index mineral reactions, such as the genesis of sillimanite according to the continuous reaction:

$$\text{biotite} + \text{pyrite} + \text{graphite} = \text{K-feldspar} + \text{sillimanite} + \text{rutile} + \text{pyrrhotite} + H_2O + CO_2 \qquad \text{(C)}$$

This formulation envisions a progressive high grade (650°-700°C, 6 kb) depletion of iron from the silicates, with biotite becoming more Mg-rich, and Fe-lacking silicates including sillimanite, becoming more abundant with increasing temperature. The progressive conversion of pyrite to pyrrhotite was further evidenced by reaction overgrowths of the latter mineral on the former. Robinson and Tracy (1977) distinguished seven assemblages in pelitic schists which arise from variation in Fe/Mg of the silicates and oxides with sulfur content; the main mineralogic events are the disappearance of garnet with progressive iron depletion, followed by rutile replacing ilmenite. The most sulfur-rich assemblages contain py-

rite–biotite–cordierite–rutile, with Fe/(Fe + Mg) of biotite and cordierite effectively zero. This important though brief summary documents, for the first time, the profound effect of (probably) sedimentogenous sulfur on pelite metamorphism via sulfide–silicate–oxide interactions.

Hutcheon (1979) discussed sulfide–oxide–silicate equilibria in sulfur-rich metasediments of the Proterozoic Amisk Group, central Manitoba, believed by Froese and Gasparini (1975) to have been metamorphosed near 600°C and 5.5 kb. The assemblages have combinations of pyrite, pyrrhotite, magnetite, and ilmenite, but no graphite. The assemblages define the vapor phase including fugacities of sulfur and oxygen, in equilibrium with the sulfide, silicate, and oxide minerals. Partial pressure of H_2O was nearly equal to total pressure during the metamorphism. The iron contents of biotite, staurolite, and chlorite steadily decrease with increasing sulfur fugacity. As in the Paxton Schist, assemblages with pyrite but not pyrrhotite have the least ferroan silicates. Garnet in these assemblages has as much as 8 wt percent MnO and staurolite as much as 5 wt percent ZnO. It is likely that these minerals are stabilized to high grade and against iron depletion by their unusual compositions.

The most thorough analysis available of sulfide–silicate–oxide interactions is that of Nesbitt (ms), some of which is reproduced in Nesbitt and Kelly (1980). He described in great detail the assemblages and compositions of sulfide-bearing pelitic schists and graywackes of the Late Precambrian Ocoee Series in the southern Appalachians near Ducktown, Tenn. The rocks have been subjected to middle grade metamorphism of probable Taconic age, with peak conditions estimated from the major mineralogy to have been 540° ± 30°C and 6 kb ± 1 kb. A distinctive series of mineral zonations is encountered, produced by increasing activity of sulfur and increasing oxygen fugacity, represented generally as follows:

1. Graphite, abundant in pyrrhotite-bearing pelitic country rocks, disappears as Fe/(Fe + Mg) starts to decrease, usually less than 100 m from an ore body.

2. Closer to the ore zones ilmenite gives way to rutile, and chlorite appears, interleaved with biotite and muscovite. In contrast to previous workers in the area, Nesbitt thought the chlorite was primary and prograde, based on habit, systematic Fe and Mg distribution with biotite ($K_{D,Fe\text{-}Mg/Bio\text{-}Chl} = 1.10$), and oxygen isotope data.

3. Staurolite disappears close to the ore bodies.

4. Garnet disappears a few meters from the ore bodies. At this point it contains up to 68 mole percent of spessartine.

5. Very close to the ore bodies pyrite is present. Nesbitt (ms) regarded it as primary, although patchy development of secondary pyrite and marcasite replacing pyrrhotite is common as a weathering phenomenon.

6. Biotite and chlorite survive into the ore zones where they are associated with pyrrhotite, pyrite, magnetite, sphene, and occasionally anhydrite and an andradite garnet.

Limits on sulfur and oxygen fugacities are defined by the Ti oxides and pyrrhotite–pyrite relations. Nesbitt estimated f_{S_2} increasing from

10^{-8} to 10^{-3} bars and f_{O_2} from 10^{-22} to 10^{-18} bars as the ore bodies are approached. Approximate calculations on the expected Fe contents of ferromagnesian silicates at 550°C and 6 kb and the above sulfur and oxygen fugacities showed that the silicates are in oxidation and sulfidation equilibrium with the oxide and sulfide minerals.

In summary, it is apparent from recent field work that a few percent of sulfur in metasediments can exert powerful controls over the silicate and oxide mineralogy, at least in the middle and higher grades, with determination of the Ti oxide minerals (ilmenite versus rutile) present, stabilization of chlorite to high grade, determination of the presence or absence of staurolite and garnet, and, possibly, aluminum silicate, and of possible unusual compositions of minerals. The succession of index minerals and the isogradic reactions producing them may be different from progressive metamorphism of less sulfidic pelites.

Recent experimental work on the stabilities of Mg–Fe amphibole (Popp, Gilbert, and Craig, 1977) and of biotite (Tso, Gilbert, and Craig, 1979) as functions of f_{O_2} and f_{S_2}, along with theoretical analysis of vapor-phase thermodynamics in the system C–O–H–S (Eugster and Skippen, 1967; Ohmoto and Kerrick, 1977) and description of methods of calculation and display of the oxygen and sulfur fugacities (Holland, 1959, 1965; Froese, 1971, 1977; Thompson, 1972), provide powerful tools for the analysis of the sulfide–silicate–oxide relations in progressive metamorphism and encourage more detailed studies of field occurrences.

Area and scope of present work.—The Anakeesta Formation of probable late Precambrian depositional age (Hadley and Goldsmith, 1963) crops out extensively in the southern Appalachians of Tennessee and North Carolina. In the Fontana Lake area several kilometers west of Bryson City, N.C., on the southeastern edge of the Great Smoky Mountains National Park, the formation is composed largely of sulfide- and graphite-rich, black to gray metashales which show a Barrovian metamorphic gradation from the garnet zone through the kyanite zone. The metamorphism is of probable Taconic age and appears to represent a single major event (Butler, 1972). The entire Barrovian sequence embraces all the allocthonous (Hatcher, 1978) Great Smoky Group, of which the Anakeesta Formation is a member, and culminates in sillimanite-bearing rocks southeast of Bryson City (Carpenter, 1970). The sulfide-rich portion of the Anakeesta Formation considered here is confined to the axis of the Murphy Syncline (fig. 1) which strikes southwestward into northern Georgia. The sulfidic schists of the Fontana Lake area were first correlated with the Anakeesta Formation, which underlies some of the high Great Smoky Mountain area north of Fontana Lake, by Hadley and Goldsmith (1963). Underlying the Anakeesta Formation is a massive graywacke sequence, the Thunderhead Formation, which exhibits monotonous quartz–feldspar–biotite mineralogy; conformably overlying the Anakeesta are the Ammons, Grassy Branch, and higher formations (Mohr, 1973) which are mainly sulfide- and graphite-poor, well-oxidized light-colored schists and metasandstones. Staurolite occurs occasionally in the

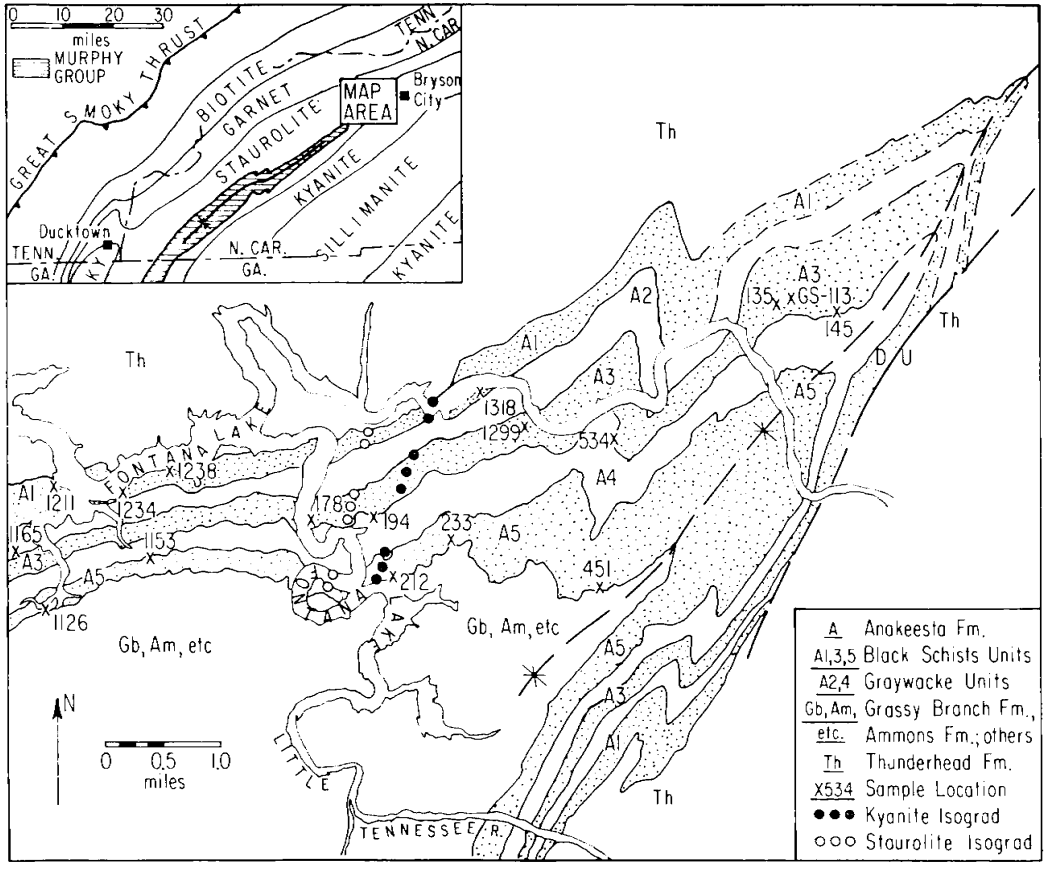

Fig. 1. Outcrop of the Anakeesta Formation in the Fontana Lake, N.C. area and locations of samples studied.

Dean Formation west of the prolongation of the staurolite isograd from the Anakeesta Formation (fig. 1); the mineralogy of intervening formations does not allow formation of staurolite. Carpenter's (1970) regional staurolite isograd passes well to the west of where staurolite appears in the Anakeesta Formation. The highest metamorphism reached in the Anakeesta black and gray schists is well into the kyanite zone. Details of the stratigraphy and structure of the area are given by Mohr (1973). The regional geology is described by Hadley and Goldsmith (1963).

The sulfidic shales of the Anakeesta Formation contain staurolite and kyanite isograds (fig. 1). The suddenness of appearance of these index minerals, together with profound associated mineralogic changes, to be described, indicates low variance of the staurolite- and kyanite-producing reactions. Associated recrystallization of pyrrhotite and its segregation into coarse veins, especially with kyanite in the darkest shales, indicate strongly that fluids played an important part in the metamorphism. Graphite is a ubiquitous accessory in all shales, which, with the absence of magnetite, implies reduced metamorphic fluids (Froese, 1971) for all the Anakeesta rocks. The sulfidic pelite metamorphism thus differs from other described areas in being lower grade than the central Massachusetts, Maine, or Manitoba localities, in having graphite throughout, in contrast to the Ducktown area, in having a low CaO tenor, in contrast to occurrences in the Sanbagawa belt and the central Alps (Frey, 1978), and in lacking primary pyrite, which is different from most of the other occurrences. In addition, the discrete nature of the sedimentary strata which embrace a range of metamorphic grade and the sharpness of the isogradic traces in the present occurrence afford a somewhat unique opportunity to study Barrovian metamorphism in the sulfidic context.

LITHOLOGY AND SAMPLE SELECTION

Five mapable units occur within the Anakeesta Formation in the Fontana Lake Area (fig. 1). These include three black schist sequences, A1, A3, and A5, separated by two units dominantly of felsic graywackes, units A2 and A4. The black schists contain numerous thin graywacke interbeds. At their contacts with the major graywacke units, black sulfide- and graphite-rich schists grade into gray schists less rich in opaque minerals. Although a few specimens were found that were transitional between black and gray schists, the great majority of schist specimens could be unambiguously classified as black or gray. Individual beds may often be traced for several kilometers along strike, but gradual change of sedimentary facies along strike is common.

Of the various additional lithologies in the Anakeesta Formation (Mohr, 1973), one group is found exclusively in black mica schist and appears to be directly involved in reactions forming kyanite. These are occasional small, gray to black pods and lenses which, within the garnet zone, are composed almost entirely of chlorite and quartz, with abundant graphite and pyrrhotite. Textural variants include schist, granofels, and metagraywacke with obvious quartz clasts. Within the kyanite zone these

are converted to quartz–biotite gneisses. Their origin is not clear; they may be metasomatized rocks originally rich in carbonate.

Figure 1 shows the locations of analyzed samples. Numbers 1211, 1153, 1238, 194, 212, 1299, 135, and GS-113 are black schists; numbers 1126, 1165, 534, and 233 are gray schists, numbers 145, 451, and 1318 are intermediate in color between gray and black; and numbers 1234 and 178 are quartz–chlorite rocks. The samples are grouped in the tables as garnet zone rocks and staurolite–kyanite zone rocks. The highest metamorphic grade exposed was sampled (specimens 135 and GS-113); outcrops of the Anakeesta Formation at higher than kyanite grade are not presently known.

A minority of the samples are from deep road cuts in the staurolite–kyanite zone. These are very fresh specimens showing preservation of the easily-weathered sulfides. Other samples are from relatively fresh outcrops along the shores of Fontana Reservoir where high-level filling has washed away the normally heavy topsoil. The sulfides in these samples are variably to completely degraded, but other minerals are normally unaltered.

PETROLOGY

Black schists.—In the more recrystallized, higher grade rocks, black schists contain a maximum of 5 to 7 modal percent of pyrrhotite plus graphite. In general, accurate modal analysis of the samples was not possible because of local segregation of aluminosilicates and sulfides into veins, very large porphyroblasts of kyanite and staurolite, and fine-grained minerals often impossible to resolve microscopically in the lower-grade rocks. Table 1 gives the qualitative mineralogy of key samples.

At low grade, black schists are made up principally of muscovite, quartz, chlorite, plagioclase, small garnet euhedra, and opaques. Paragonite occurs in some of the lower-grade black schists but never with plagioclase. Rutile is the only oxide mineral. A few samples show pseudomorphs of rutile after ilmenite. Graphite occurs as unresolvable "dust."

Kyanite development takes place in the black schists over a zone at least 1 km wide. The first changes in mineralogy include appearance of millimeter-size biotite porphyroblasts within the black schists and the sparse occurrence of small hydrothermal veins containing kyanite, white mica, and quartz. Matrix chlorite remains a constituent of the black mica schist. This region is termed the "transition zone."

The actual kyanite isograd is marked by the appearance of sparse, centimeter-size kyanite crystals within black mica schist along with both porphyroblastic biotite and matrix chlorite. Over a distance of a few hundred meters upgrade, kyanite and biotite increase in abundance until matrix chlorite has disappeared. Retrograde alteration of biotite to chlorite and of kyanite to white mica and chlorite is extensive within the "transition zone" and at the kyanite isograd.

In some beds of black mica schist, no further changes are seen once matrix chlorite has disappeared. The kyanite-zone assemblage is quartz–muscovite–biotite–kyanite (in crystals up to several cm long)–Mn-rich garnet–matrix plagioclase–rutile–graphite–pyrrhotite. X-ray diffraction

TABLE 1

Mineral assemblages of analyzed samples

	GARNET AND TRANSITION ZONES							STAUROLITE-KYANITE ZONE										
	Gray Schists		Black Schists					Gray Schists		Inter. Schists			Black Schists			Quartz-Chlorite Rocks		
Sample number	1126	1165	1153	1211	1238	194	212	233	534	145	451	1318	1299	GS-113	135	1234	1238a	178
Quartz	X	X	X	X	X	X	X	X	X	X	X	X	X	X	X	X	X	X
Muscovite	X	X	X	X	X	X	X	X	X	X	X	X	X	X	X			
Paragonite				X	X								X	X	X			
Biotite	P	X				P	P	P	P	P	P	P	P	P	P			P
Chlorite	X	X	X	X	X	X	X	R	R	R	R	R	R	R	R	X	X	X
Garnet	P	P	P	P	P	P	P	P	P	P	P	P	P	P	P	P		P
Staurolite								P	P	P	P	P						
Kyanite										P	P	P	P	P	P			
Plagioclase	X	X	X			X	X	X	X	X	X	X	P	P	P			
Ilmenite	X	X	a					X	X	X	X	X						
Rutile			X[b]	X	X	X	X[b]		X	X	X	X	X	X	X			
Sphene																X	X	X
Graphite	X	X	X	X	X	X	X	X	X	X	X	X	X	X	X	X	X	X
Pyrrhotite	*	*	*	*	*	*	*	X	X	X	*	*	*	X	X	*	*	*

Apatite present in all rocks; tourmaline and zircon present in all mica schists.

X Prograde mineral, matrix.

P Prograde mineral, porphyroblastic.

R Retrograde mineral.

* Pyrrhotite originally present in all rocks, but commonly weathered out or altered to supergene pyrite.

a Ilmenite armored by garnet.

b Rutile pseudomorphic after ilmenite.

PLATE I

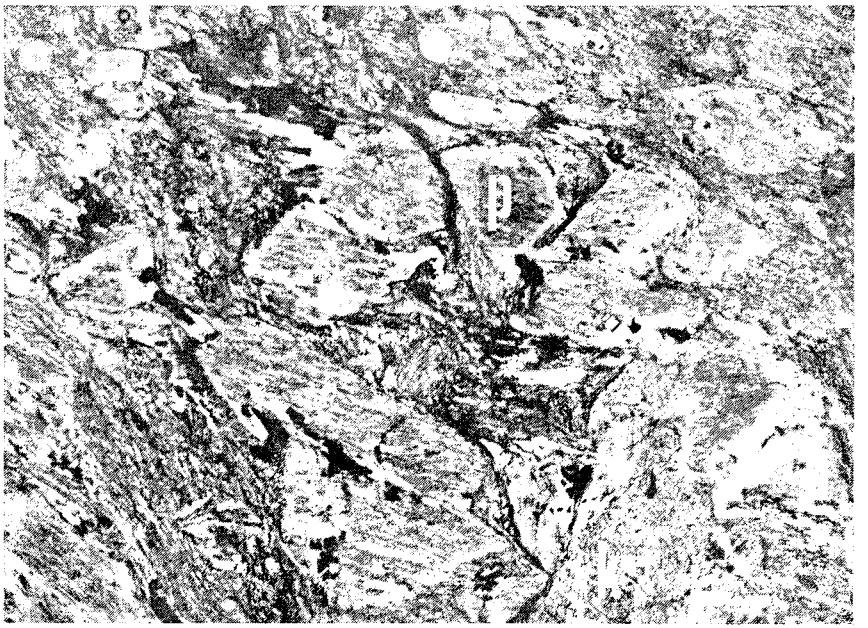

Photomicrograph of black schist 135. Plagioclase (p), kyanite (k) and biotite (b) porphyroblasts labelled. A few small garnet euhedra with thin rims are near the top edge. Note thin inclusion-free, Na-rich rims of plagioclase. Dark matrix material is pyrrhotite and graphite. Plagioclase grain labelled "p" is 1 mm across.

studies of white mica show paragonite to be absent in these monotonous black schists.

Other beds of black mica schist, such as that shown in plate 1, show additional changes in mineralogy, beginning about 1 km east of the kyanite isograd. Plagioclase occurs as large, spongy oligoclase porphyroblasts, often with thin, inclusion-free rims of more sodic plagioclase. Kyanite increases in abundance and size, with crystal length up to 10 cm. X-ray diffraction studies of white mica show the frequent occurrence of paragonite as a separate phase, apparently in equilibrium with both plagioclase and biotite. There is evidence that this higher-grade paragonite exsolved from muscovite in a post-kyanite prograde event.

Features common to all black mica schists within the kyanite zone are the following. Garnets remain very small and few, but some show definite euhedral overgrowths on earlier cores (pl. 1). Pyrrhotite shows a strong tendency to segregate into veins that also contain quartz, and in some cases kyanite or chlorite. Graphite is recrystallized into tiny plates, just resolvable with the petrographic microscope. Chlorite is ubiquitous as retrogressive replacement of kyanite and, in some rocks, as millimeter-size ovoid spots which may be retrogressive pseudomorphs after biotite. Matrix chlorite does not occur. Staurolite is never found in the black mica schists.

Quartz–chlorite rocks.—Although they are minor in amount, the quartz–chlorite rocks are petrologically distinct. They are commonly rich in sulfide and graphite. Sphene is the characteristic Ti-mineral. Apatite in long, slender crystals is common. Large Ca- and Mn-rich garnets were found in some quartz–chlorite rocks, as in no. 178. About 1 km below the kyanite isograd, the quartz–chlorite rocks develop biotite porphyroblasts. At higher grades they are converted to quartz–biotite gneisses. Retrograde effects in these rocks are limited to occasional, slight replacement of biotite by chlorite.

Gray schists.—These beds are markedly lower in graphite and pyrrhotite than the black schists, with generally less than 2 percent of opaques. They contain nearly the same minerals at lower grades as the black schists, with a few differences. Biotite is prevalent, paragonite is absent, and ilmenite is the oxide mineral rather than rutile, in the form of platelets up to 0.25 mm across. Garnets are larger and more numerous than in the black schists. They tend to be filled with quartz and plagioclase inclusions and may make up 2 percent of the mode in some rocks. Biotite can be both porphyroblastic and in the matrix and is more pleochroic than in the black schists. Chlorite occurs in the fine-grained matrix and, in some specimens, as retrogressive alterations of biotite and garnet. It is distinctly pleochroic in greens with low anomalous interference colors.

The staurolite isograd in the gray schists is abrupt. Staurolite as inclusion-filled porphyroblasts up to 10 cm across appears suddenly, with complete loss of matrix chlorite, partial conversion of ilmenite to rutile in some rocks, and possible slight growth of garnet and biotite. Staurolite is commonly patchily retrogressed to white mica and chlorite. Kyanite was not produced in the gray schists.

A few higher grade rocks were found which are intermediate between gray schists and black schists. These have 2 to 4 modal percent of sulfide and graphite, both kyanite and staurolite, and discrete ilmenite and rutile. Garnets are intermediate in size and amount between those of black schists and gray schists.

METHODS OF CHEMICAL ANALYSIS

Whole rock analysis.—Eight black and gray schists were analyzed for major element oxides, CO_2, total sulfur, total carbon, and selected minor elements (table 2). The analyses were made by X-ray Assay Lab, Don Mills, Ontario, and were by X-ray fluorescence, except for CO_2, which was analyzed by a titration method. Iron is recorded in table 2 as FeO, although much of the iron determined by XRF is in the form of FeS. A first-order correction may be applied to the spectroscopic values based on the sulfur contents, where the analyses for S are reliable, and on the average pyrrhotite composition of $Fe_{0.85}S$ determined by microprobe analysis of some black schists; this method assumes negligible Fe_2O_3 content, which is indicated by the abundant graphite and absence of magnetite in all of the rocks analyzed.

TABLE 2
Rock analyses (X-ray Assay Laboratories)

	GARNET AND TRANSITION ZONES			STAUROLITE-KYANITE ZONE				
	Gray Schists	Black Schists		Gray Schists	Intermediate Schists		Black Schists	
wt. %	1126	1153	1211	534	1318	145	1299	GS-113
SiO_2	55.3	54.4	53.4	55.7	55.5	44.5	58.5	56.6
Al_2O_3	22.6	25.7	28.3	23.0	22.3	29.1	20.4	22.5
CaO	0.27	0.17	0.78	0.26	1.57	0.74	1.81	0.49
MgO	1.85	2.28	2.29	2.08	3.28	3.48	2.68	2.62
Na_2O	0.33	0.72	2.43	0.52	1.27	1.61	1.36	2.11
K_2O	5.49	5.79	3.56	5.94	3.67	5.42	3.74	3.71
FeO	4.9	1.5	0.8	4.6	3.3	6.0	2.4	4.3
FeO*	6.72	2.52	1.49	6.80	6.27	7.07	4.14	4.73
MnO	0.18	0.11	0.18	0.18	0.15	0.10	0.89	0.17
TiO_2	0.77	0.88	0.84	0.74	1.01	1.33	0.56	0.65
P_2O_5	0.18	0.11	0.13	0.18	0.24	0.26	1.18	0.13
L.O.I.	3.54	4.62	5.54	2.47	3.39	3.92	3.93	4.54
CO_2	0.2	0.1	0.1	0.2	0.1	0.3	0.2	0.1
C	0.10	0.62	1.30	0.17	0.35	0.59	0.35	0.83
S	0.01	nil	nil	0.42	1.11	1.32	1.09	1.83
ppm								
Cl	1000	850	1000	200	700	1000	400	800
Cr_2O_3	110	240	180	130	200	190	190	140
Zr	80	180	130	130	200	210	120	90
Sr	160	100	300	80	120	130	150	320
Rb	210	100	110	190	160	160	150	140

L.O.I. = Loss on ignition.
FeO = FeO by wet chemical analysis.
FeO* = Total Fe (by spectroscopy) as FeO.

TABLE 3

Analyses of white micas

	GARNET AND TRANSITION ZONES							STAUROLITE-KYANITE ZONE							
	Gray Schists		Black Schists					Gray Schists		Inter. Schists			Black Schists		
Sample number	1126	1165	1153	1211*	1238*	194	212	233	534	145	451	1318	1299*	GS-113*	135*
Procedure used	EDS	EDS	Spec	EDS	EDS	Spec	Spec	Spec	Spec	EDS	EDS	EDS	Spec	EDS	Spec
Wt. % oxides															
Na_2O	1.06	0.93	1.13	1.52	1.49	1.02	1.26	1.62	1.43	1.50	1.74	0.99	2.31	2.06	2.32
MgO	0.74	0.76	0.95	0.61	1.00	1.33	1.03	0.48	0.48	1.41	0.42	1.22	0.58	1.28	0.77
Al_2O_3	34.90	34.56	33.43	36.40	36.46	33.08	33.60	35.62	35.96	34.91	36.85	35.00	35.80	36.70	34.38
SiO_2	47.57	47.57	47.78	46.69	47.08	47.72	48.38	46.45	46.12	45.54	46.11	45.71	47.22	46.82	46.95
K_2O	9.86	9.83	9.67	8.70	9.27	9.53	9.26	8.82	9.57	8.75	8.55	9.13	8.34	7.95	7.88
CaO	0.00	0.00	0.03	0.05	0.00	0.02	0.01	0.02	0.02	0.00	0.04	0.15	0.02	0.00	0.09
TiO_2	0.15	0.17	0.35	0.24	0.20	0.40	0.42	0.31	0.47	0.67	0.49	0.41	0.40	0.72	0.90
MnO	0.03	0.02	0.03	0.03	0.00	0.02	0.01	0.00	0.00	0.00	0.01	0.00	0.00	0.00	0.00
FeO	1.58	1.44	0.96	0.16	0.18	0.81	0.94	1.00	0.70	0.56	0.60	0.73	0.60	0.00	0.42
Total oxide	95.94	95.28	94.33	94.40	95.77	93.93	94.92	94.32	94.75	93.34	94.79	93.34	95.27	95.53	93.72
Atoms/22 oxygens															
Si	6.27	6.30	6.38	6.18	6.16	6.39	6.40	6.19	6.14	6.08	6.10	6.16	6.21	6.11	6.27
Al	1.73	1.70	1.62	1.82	1.84	1.61	1.60	1.81	1.86	1.92	1.90	1.84	1.79	1.89	1.73
IV	8.00	8.00	8.00	8.00	8.00	8.00	8.00	8.00	8.00	8.00	8.00	8.00	8.00	8.00	8.00
Al	3.69	3.70	3.64	3.85	3.79	3.61	3.64	3.78	3.78	3.68	3.84	3.72	3.76	3.76	3.68
Ti	0.02	0.02	0.04	0.02	0.02	0.04	0.04	0.03	0.05	0.07	0.05	0.04	0.04	0.07	0.09
Mg	0.15	0.15	0.19	0.12	0.20	0.27	0.20	0.09	0.10	0.28	0.08	0.25	0.11	0.25	0.15
Mn	0.00	0.00	0.00	0.00	0.00	0.00	0.00	0.00	0.00	0.00	0.00	0.00	0.00	0.00	0.00
Fe	0.17	0.16	0.11	0.02	0.02	0.09	0.11	0.11	0.08	0.06	0.07	0.08	0.07	0.00	0.05
VI	4.03	4.03	3.98	4.01	4.03	4.01	3.99	4.01	4.01	4.09	4.04	4.09	3.98	4.08	3.97
Na	0.27	0.24	0.29	0.39	0.38	0.27	0.32	0.42	0.37	0.39	0.45	0.26	0.59	0.52	0.60
K	1.66	1.66	1.65	1.47	1.55	1.63	1.56	1.50	1.62	1.49	1.44	1.57	1.40	1.32	1.34
Ca	0.00	0.00	0.00	0.01	0.00	0.00	0.00	0.00	0.00	0.00	0.01	0.02	0.00	0.00	0.01
XII	1.93	1.90	1.94	1.87	1.93	1.90	1.88	1.92	1.99	1.88	1.90	1.85	1.99	1.84	1.95
Na/K+Na	0.14	0.13	0.15	0.21	0.20	0.14	0.17	0.22	0.19	0.21	0.24	0.14	0.30	0.28	0.31
Mg/Mg+Fe	0.47	0.48	0.63	0.86	0.91	0.75	0.65	0.45	0.56	0.82	0.53	0.76	0.61	1.00	0.75
Percent celadonite derived from:															
Mg+Fe	16	16	15	7	11	18	16	10	9	17	8	17	9	12	10
Si	14	15	19	9	8	20	20	10	7	4	5	8	11	6	14
Total Al	15	15	19	8	9	20	19	10	9	10	7	11	11	9	15

* X-ray diffraction shows intergrown muscovite and paragonite.

Mineral analyses.—Minerals of 18 rocks were analyzed by electron microprobe. The analyses were performed over a period of 10 yrs in four different localities. The first analyses were by crystal spectrometers on the Chicago ARL microprobe in 1970. More analyses were made at Virginia Polytechnic Institute in 1972-1973 with their ARL-spectrometer instrument. Some analyses were made by R. A. Barnett at the University of Western Ontario in 1980 on a MAC instrument with energy-dispersive measurement. Finally, previous analyses were checked and new ones obtained with the Chicago ARL-EDS system in 1980. Mineral analyses are presented in tables 3 through 9.

The compositions of white mica and pyrrhotite were estimated by X-ray diffraction scans at 1/8° 2θ per min with CuKα radiation and internal standards of natural quartz and synthetic annealed BaF_2 and corundum, using calibrations based on the (0, 0, 10) reflection of white mica (Zen and Albee, 1964; Guidotti, 1970) and the (102) reflection of pyrrhotite (Toulmin and Barton, 1964).

MINERALOGY

White mica is, after quartz, the most widespread schist mineral. In many samples of black schist, muscovite is intimately intergrown with paragonite, and independent microprobe analyses of these two phases were not possible, except for a few large retrogressive white micas. In these samples, composition of muscovite and paragonite was determined by X-ray diffraction. Where matrix muscovite occurs without paragonite,

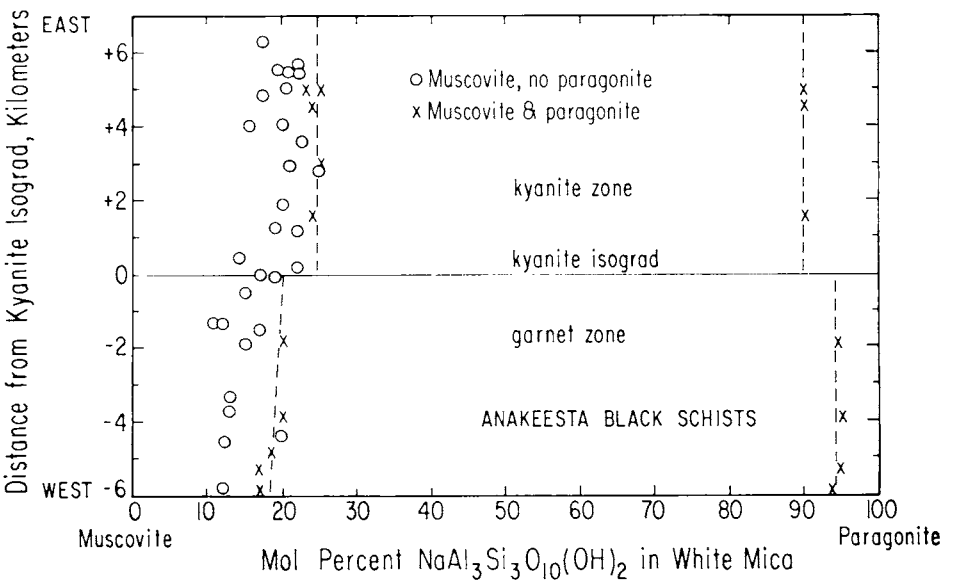

Fig. 2. Compositions of muscovite and paragonite in black schists as functions of distance along strike from the kyanite isograd (fig. 1), determined by X-ray diffraction. Note apparent discontinuities at isograd.

reliable microprobe analyses were obtained. These agree with the X-ray diffraction analyses to within 1 mole percent $KAl_3Si_3O_{10}(OH)_2$. Analyses of muscovites are given in table 3. All white micas are close to the expected stoichiometries, except for a possible very slight alkali deficiency.

Figure 2 shows the X-ray determinations of compositions of muscovite and paragonite in black schists as a function of distance normal to the kyanite isograd. An abrupt narrowing of the muscovite–paragonite solvus is evident at the isograd. There is some indication that the mafic components simultaneously decrease from a celadonite mol fraction of 15 to 18 percent to less than 12 percent at the kyanite isograd, though Mg and Fe analyses show considerable scatter. The discontinuous changes in white mica compositions at the kyanite isograd are not obviously explainable by equilibrium considerations. It is possible that compositions are metastable in the garnet zone but have changed to near-equilibrium compositions in the presence of abundant hydrous flux released in the kyanite-forming event. Alternatively, paragonite in lower-grade black schists may contain some margarite molecule, which would affect the K, Na distribution between muscovite and paragonite, as found by Thompson, Lyttle, and Thompson (1977) in plagioclase-free schists from Gassetts, Vt. Microprobe scans of unresolvable muscovite–paragonite intergrowths in black schists 1211 and 1238 (table 3) did not reveal substantial quantities of Ca, however.

A temperature of about 600°C results from the application of the Eugster and others (1972) experimental muscovite–paragonite solvus to the post-kyanite black schists, using either the Na-rich or the K-rich limb. Eugster and others (1972) gave reasons based on field petrology why their solvus may yield temperature estimates that are somewhat too high, and this point has been raised by others, for example Rumble (1978). Thus the figure of 600°C should be regarded as an upper temperature limit for the staurolite–kyanite metamorphism.

Biotite.—Table 4 presents selected biotite analyses. The most noteworthy feature is the great spread of Mg/(Mg + Fe) values, ranging from 0.33 in some garnet-zone gray schists to 0.82 in the darkest black schists. There is a jump from 0.3—0.4 to 0.5—0.6 in gray schists at the staurolite isograd. Most of the analyses are considerably more aluminous than predicted by the phlogopite–annite–eastonite–siderophyllite model, with 0.3 to 0.5 Al per 22 oxygen in excess over eastonite–siderophyllite, and K + Na contents as low as 1.4 to 1.5 atoms per 22 oxygens. Figure 3 shows that the Al contents do not correlate with Mg/(Mg + Fe) values, as found also by Guidotti, Cheney, and Conatore (1975b), but that there is a negative correlation of alkali atoms and TiO_2 content with Mg/(Mg + Fe) values. The lowest TiO_2 contents of biotite occur in the most sulfide-rich rocks where rutile is the titanium oxide mineral.

One may ask whether the low-alkali, high-Al analyses of biotite are not merely due to chlorite contamination of the biotite, which alteration is nearly ubiquitous. Against this hypothesis are the evidences of lack of visible alteration of most of the biotites analyzed, lack of correlation of

TABLE 4
Biotite analyses

	GARNET AND TRANSITION ZONES			STAUROLITE-KYANITE ZONE								
	Gray Schists		Black Schists	Gray Schists		Intermediate Schists			Black Schists			Qtz.-Chlorite Rock
Sample number	1126	1165	212	233	534	145	451	1318	1299	GS-113	135	178
Procedure used	EDS	EDS	Spec	Spec	Spec	EDS	Spec	EDS	Spec	EDS	Spec	Spec
Wt. % oxides												
Na_2O	0.06	0.00	0.26	0.32	0.35	0.00	0.36	0.00	0.30	0.00	0.28	0.14
MgO	7.24	8.08	14.73	11.28	11.65	13.23	12.92	13.27	16.28	17.78	18.27	17.23
Al_2O_3	18.72	18.43	17.55	19.32	19.67	19.36	19.76	19.75	20.02	20.43	19.87	18.36
SiO_2	35.86	35.67	38.92	36.08	36.94	36.86	37.25	37.11	38.08	40.02	39.55	37.59
K_2O	9.06	8.94	8.58	8.76	8.51	8.56	8.48	8.31	7.77	7.88	7.79	7.92
CaO	0.00	0.00	0.02	0.00	0.02	0.00	0.00	0.00	0.00	0.00	0.00	0.04
TiO_2	1.83	1.68	1.25	1.49	1.39	1.55	1.47	1.33	0.91	0.70	0.69	0.97
MnO	0.05	0.09	0.19	0.00	0.00	0.00	0.01	0.00	0.17	0.00	0.21	0.33
FeO	23.57	22.09	13.70	17.86	16.15	14.95	15.10	14.90	11.31	8.89	7.87	9.18
Total oxide	96.39	94.98	95.20	95.11	94.69	94.51	95.35	94.67	94.84	95.70	94.53	93.38
Atoms/22 oxygens												
Si	5.47	5.49	5.79	5.43	5.51	5.48	5.49	5.49	5.53	5.64	5.65	5.60
Al	2.53	2.51	2.21	2.57	2.49	2.52	2.51	2.51	2.47	2.35	2.35	2.40
IV	8.00	8.00	8.00	8.00	8.00	8.00	8.00	8.00	8.00	8.00	8.00	8.00
Al	0.84	0.83	0.87	0.85	0.97	0.87	0.92	0.93	0.95	1.03	0.99	0.76
Ti	0.21	0.19	0.14	0.17	0.16	0.17	0.16	0.15	0.10	0.07	0.07	0.11
Mg	1.65	1.85	2.93	2.53	2.59	2.93	2.84	2.93	3.52	3.73	3.89	3.93
Mn	0.01	0.01	0.02	0.00	0.00	0.00	0.00	0.00	0.02	0.00	0.02	0.04
Fe	3.01	2.84	1.71	2.25	2.02	1.86	1.86	1.84	1.37	1.05	0.94	1.12
VI	5.72	5.72	5.67	5.81	5.74	5.83	5.78	5.85	5.96	5.88	5.91	5.96
Na	0.02	0.00	0.08	0.08	0.09	0.00	0.10	0.00	0.09	0.00	0.08	0.04
K	1.76	1.76	1.63	1.68	1.62	1.62	1.59	1.57	1.43	1.42	1.42	1.47
Ca	0.00	0.00	0.00	0.00	0.00	0.00	0.00	0.00	0.00	0.00	0.00	0.01
XII	1.78	1.76	1.71	1.76	1.71	1.62	1.69	1.57	1.51	1.42	1.50	1.52
Mg+Mn+Fe	4.67	4.70	4.66	4.78	4.61	4.79	4.70	4.77	4.91	4.78	4.85	5.09
Mg/Mg+Fe	0.35	0.39	0.63	0.53	0.56	0.61	0.60	0.61	0.72	0.78	0.81	0.78
Total Al	3.37	3.34	3.08	3.43	3.46	3.39	3.43	3.44	3.42	3.39	3.34	3.16
Alkali deficiency	0.22	0.24	0.29	0.24	0.29	0.38	0.31	0.43	0.49	0.58	0.50	0.48

Al content with K content, and uniformity of the analyses in any given specimen. It is conceivable that the low-alkali biotites should be regarded as mixed layer biotite–chlorite minerals. Under this hypothesis, the charge deficiency due to low alkalis would be compensated by OH^- replacing O^{2-}.

Chlorite.—All analyzed chlorite (table 5) satisfies the ideal formula $(Mg, Fe)_{6-x}Al_{2x}Si_{4-x}O_{10}(OH)_8$, with Al/Si ratios within the range given by Miyashiro (1973). As with other ferromagnesian minerals, Mg/(Fe + Mg) varies widely with the sulfur content of the rocks, from 0.4 in low-grade gray schists to 0.8 in high-grade black schists. There is a distinct jump from 0.4 to 0.5—0.6 in gray schists at the staurolite isograd.

The problem of retrogressive versus prograde chlorite in high-grade schists is unresolved by critical evidence. The biotite–chlorite Fe–Mg distribution is very regular for all schists (fig. 4), in contrast to the scattered garnet–chlorite and white mica–chlorite distributions, and no compositional distinction can be made between obviously retrogressive chlorite which replaces biotite in samples 194 and 212 and associated matrix chlorite. Matrix chlorite has not been identified in schists of staurolite–kyanite grade. The change in mode of occurrence of chlorite above the staurolite and kyanite isograds, as well as thermodynamic lines of argu-

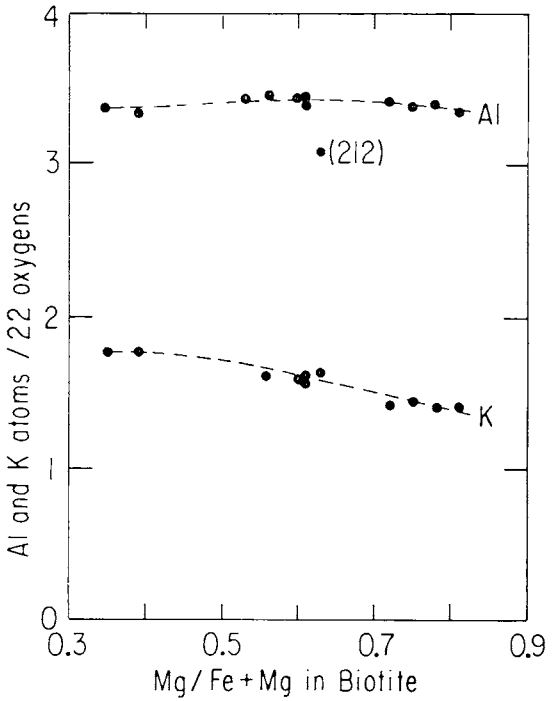

Fig. 3. Al and K contents of gray and black schist biotites. Note independence of Al and dependence of K on Fe content.

TABLE 5

Analyses of chlorite

	GARNET AND TRANSITION ZONES							STAUROLITE-KYANITE ZONE							
	Gray Schists		Black Schists					Gray Schists		Inter. Schists			Black Schists		Qtz.-Chl. Rock
Sample number	1126	1165	1153	1211	1238	194	212[k]	233[b]	534[b]	145[b]	451[st]	1318[b]	1299[b]	135[k]	178
Procedure used	EDS	EDS	Spec	EDS	EDS	Spec	Spec	Spec	Spec	EDS	Spec	EDS	Spec	Spec	Spec
Wt. % oxides															
MgO	10.58	11.84	18.01	20.78	22.64	23.28	19.55	16.41	17.38	19.81	16.77	18.62	21.99	24.84	24.04
Al_2O_3	21.48	21.24	23.95	25.13	24.97	24.17	23.32	23.56	23.72	24.74	24.26	24.35	24.88	24.75	23.16
SiO_2	25.28	24.59	26.26	27.57	27.83	27.72	25.60	24.93	25.14	26.54	25.06	25.84	26.89	27.48	27.11
CaO	0.00	0.00	0.02	0.00	0.00	0.01	0.01	0.00	0.00	0.00	0.01	0.00	0.01	0.00	0.03
TiO_2	0.10	0.12	0.06	0.00	0.00	0.04	0.11	0.04	0.03	0.00	0.03	0.00	0.08	0.06	0.05
MnO	0.13	0.18	0.54	0.80	0.97	0.40	0.36	0.01	0.01	0.00	0.19	0.00	0.32	0.35	0.53
FeO	30.71	29.54	20.23	13.19	11.00	12.57	17.84	22.91	21.03	18.78	21.40	18.79	14.08	9.36	11.88
Total oxide	88.28	87.51	89.07	87.46	87.39	88.19	86.78	87.86	87.72	89.87	87.72	87.60	87.85	86.84	86.80
Atoms/14 oxygens															
Si	2.72	2.66	2.62	2.71	2.71	2.70	2.62	2.58	2.58	2.62	2.58	2.62	2.66	2.68	2.68
Al	1.28	1.34	1.38	1.29	1.29	1.30	1.38	1.42	1.42	1.38	1.42	1.38	1.34	1.32	1.32
IV	4.00	4.00	4.00	4.00	4.00	4.00	4.00	4.00	4.00	4.00	4.00	4.00	4.00	4.00	4.00
Al	1.44	1.36	1.46	1.63	1.58	1.46	1.43	1.46	1.45	1.49	1.52	1.53	1.51	1.52	1.39
Ti	0.01	0.01	0.01	0.00	0.00	0.00	0.01	0.00	0.00	0.00	0.00	0.00	0.01	0.01	0.00
Mg	1.69	1.89	2.70	3.05	3.29	3.38	2.98	2.53	2.72	2.91	2.57	2.81	3.24	3.61	3.55
Mn	0.01	0.02	0.05	0.07	0.08	0.03	0.03	0.00	0.00	0.00	0.02	0.00	0.03	0.03	0.04
Fe	2.76	2.67	1.70	1.09	0.90	1.02	1.53	1.98	1.81	1.55	1.84	1.59	1.17	0.76	0.98
VI	5.91	5.95	5.92	5.84	5.85	5.89	5.98	5.97	5.98	5.95	5.95	5.93	5.96	5.93	5.96
Mg/Mg+Fe	0.38	0.41	0.61	0.74	0.79	0.77	0.66	0.56	0.60	0.65	0.58	0.64	0.73	0.83	0.78
Mg+Mn+Fe	4.46	4.58	4.45	4.21	4.27	4.43	4.54	4.51	4.53	4.46	4.43	4.40	4.44	4.40	4.57
Total Al	2.72	2.70	2.84	2.92	2.87	2.76	2.81	2.88	2.87	2.87	2.94	2.91	2.85	2.84	2.71
Departure of Al from ideal formula, based on Mg+Mn+Fe															
	-0.26	-0.14	-0.26	-0.66	-0.59	-0.38	-0.11	-0.10	-0.07	-0.21	-0.20	-0.29	-0.27	-0.36	-0.15

Probably retrograde after biotite (b), staurolite (st), or kyanite (k).

ment, suggest that all chlorite within the staurolite–kyanite zone is retrograde. If so, the constant value of $K_{D(Fe\text{-}Mg/Bio\text{-}Chl)}$ suggests that this retrograde event occurred at temperatures nearly as high as the thermal peak of metamorphism.

Garnet.—The iron depletion of silicates is seen most clearly in garnet compositions. The most sulfide-rich black schists have garnet with 50 to 60 mole percent spessartine: the small sizes and amounts indicate that the garnets are present only because of stabilization by Mn. Large complementary grossular contents are characteristic. Tables 6 and 7 give the analyses.

Figure 5 shows the close relationship between garnet compositions and compositions of coexisting biotites in staurolite–kyanite grade schists. Such a strong correlation between the Mg/(Mg + Fe) ratios of the biotites and the Mn contents of the coexisting garnets was also found by Nesbitt (ms); these features are in turn strongly correlated with sulfur contents

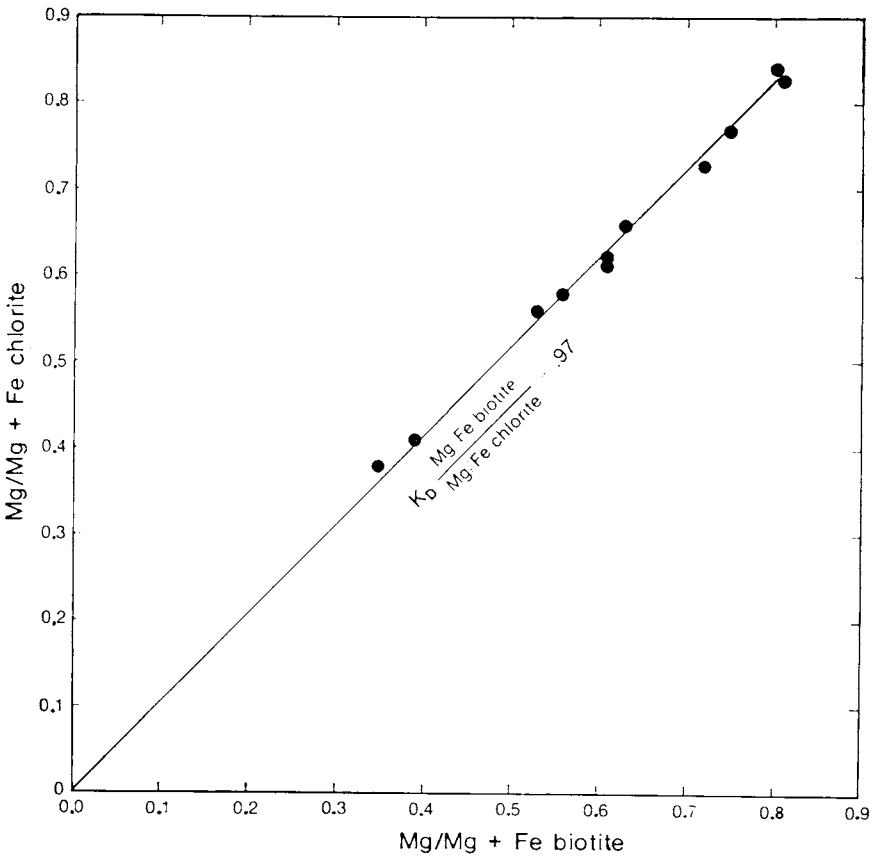

Fig. 4. Distribution of Fe and Mg between coexisting chlorite and biotite for gray and black schists of garnet *and* staurolite–kyanite zones. Note apparent lack of grade dependence.

TABLE 6

Garnet analyses, garnet and transition zones

	Gray Schists				Black Schists										Qtz-Chl Rock	
Sample number	1126		1165		1153		1211		1238		194		212		178	
Procedure used	EDS		EDS		Spec		EDS		EDS		Spec		Spec		Spec	
	core	rim	core	rim	core	rim	core	rim	core	rim	core	rim	core	rim	core	rim
Wt. % oxides																
MgO	0.77	1.41	1.48	1.52	1.61	1.83	1.46	2.43	2.02	2.16	2.61	2.99	1.55	2.96	1.44	2.81
Al_2O_3	21.85	21.59	21.52	21.54	22.58	22.13	21.46	21.43	21.01	21.43	22.00	22.36	21.73	21.73	21.62	22.05
SiO_2	37.24	37.35	36.99	36.39	37.54	37.75	37.86	38.17	36.93	37.78	37.49	38.26	37.48	38.03	37.72	37.78
CaO	2.68	2.64	2.83	2.40	3.72	3.49	2.43	2.23	2.13	2.14	2.31	3.55	4.78	2.18	7.78	4.79
MnO	11.95	4.18	6.58	5.13	19.31	15.95	26.24	22.06	24.89	24.15	21.78	17.67	17.92	11.32	22.18	17.52
FeO	26.49	32.59	29.64	31.70	16.50	20.05	11.04	14.70	11.35	12.22	13.55	16.85	16.50	24.57	10.27	16.41
Total oxide	100.98	99.76	99.04	98.68	101.26	101.20	100.49	101.02	98.33	99.25	99.74	101.68	99.96	100.79	101.02	101.36
Atoms/24 oxygens																
Si	5.98	6.03	60.1	5.96	5.95	5.98	6.06	6.06	6.03	6.10	6.00	5.99	6.01	6.03	5.97	5.95
Al	4.14	4.11	4.12	4.16	4.21	4.13	4.05	4.01	4.04	3.96	4.14	4.12	4.10	4.06	4.04	4.09
Mg	0.18	0.34	0.36	0.37	0.38	0.43	0.35	0.58	0.49	0.52	0.62	0.70	0.37	0.70	0.34	0.66
Ca	0.46	0.46	0.49	0.42	0.63	0.59	0.42	0.38	0.37	0.37	0.40	0.60	0.82	0.37	1.32	0.81
Mn	1.63	0.57	0.91	0.71	2.59	2.15	3.56	2.96	3.45	3.30	2.97	2.34	2.43	1.52	2.97	2.34
Fe	3.56	4.40	4.03	4.34	2.19	2.66	1.48	1.95	1.55	1.65	1.81	2.20	2.21	3.26	1.36	2.16
Sum of R	5.83	5.77	5.79	5.84	5.79	5.83	5.81	5.87	5.86	5.84	5.80	5.84	5.83	5.85	5.99	5.97
Pyrope	3.1	5.9	6.2	6.3	6.6	7.4	6.0	9.9	8.4	8.9	10.7	12.0	6.4	11.9	5.7	11.1
Almandine	61.0	76.2	69.6	74.3	37.8	45.6	25.5	33.2	26.4	28.3	31.2	37.7	37.9	55.8	22.7	36.2
Spessartine	28.0	9.9	15.7	12.2	44.7	36.9	61.3	50.4	58.9	56.5	51.2	40.0	41.7	26.0	49.6	39.2
Grossular	7.9	8.0	8.5	7.2	10.9	10.1	7.2	6.5	6.3	6.3	6.9	10.3	14.0	6.3	22.0	13.5

Spectrometer shows < 0.2 wt % TiO_2 in any garnet.

TABLE 7

Analyses of garnets, staurolite–kyanite zone

	Gray Schists				Intermediate Schists						Black Schists					
Sample Number	233		534		145		451		1318		1299		135		GS-113	
Procedure Used	Spec		Spec		EDS		Spec		EDS		Spec		Spec		EDS	
	core	rim	core	rim	core	rim	core	rim	core	rim	core	rim	core	rim	core	rim
Wt. % oxides																
MgO	1.90	3.08	2.31	3.20	3.28	3.63	3.86	3.55	2.43	3.17	3.18	2.54	3.56	2.86	4.61	4.48
Al_2O_3	21.21	21.53	21.53	21.68	21.88	21.98	21.86	21.71	21.78	21.91	21.37	21.47	21.79	21.67	22.53	22.16
SiO_2	37.32	37.64	36.94	37.36	37.27	36.83	37.63	37.63	37.52	37.58	37.74	37.17	37.85	37.53	38.49	37.73
CaO	5.84	3.29	5.97	4.10	4.01	1.68	2.45	2.49	6.77	4.54	1.99	1.87	1.57	1.56	1.69	2.27
MnO	6.73	0.64	6.14	2.18	7.12	5.06	5.38	5.48	6.55	3.57	13.03	13.69	18.62	19.37	15.67	16.50
FeO	28.38	35.42	28.39	32.09	26.41	29.93	30.75	30.02	26.36	30.88	21.68	22.11	16.42	16.72	18.32	18.87
Total oxide	101.38	100.96	101.28	100.61	99.97	99.12	101.93	100.88	101.41	101.65	98.99	98.55	99.82	99.71	101.31	102.01
Atoms/24 oxygens																
Si	5.94	5.96	5.88	5.95	5.91	5.93	5.92	5.97	5.92	5.92	6.06	6.02	6.03	6.02	5.99	5.90
Al	3.98	4.02	4.05	4.06	4.09	4.17	4.05	4.06	4.05	4.07	4.05	4.10	4.09	4.10	4.14	4.08
Mg	0.45	0.73	0.55	0.76	0.78	0.87	0.90	0.84	0.57	0.74	0.76	0.61	0.85	0.68	1.07	1.04
Ca	1.00	0.56	1.02	0.70	0.68	0.29	0.41	0.42	1.15	0.77	0.34	0.33	0.27	0.27	0.28	0.38
Mn	0.91	0.08	0.83	0.29	0.96	0.69	0.72	0.74	0.88	0.48	1.77	1.88	2.51	2.63	2.07	2.19
Fe	3.78	4.69	3.77	4.25	3.50	4.03	4.05	3.98	3.48	4.07	2.91	2.99	2.19	2.24	2.39	2.47
Sum of R	6.14	6.06	6.17	6.00	5.92	5.88	6.08	5.98	6.08	6.06	5.78	5.81	5.82	5.82	5.81	6.08
Pyrope	7.3	12.0	8.9	12.7	13.1	14.8	14.8	14.0	9.3	12.2	13.2	10.5	14.6	11.7	18.4	17.1
Almandine	61.6	77.4	61.1	70.8	59.1	68.5	66.6	66.6	57.3	67.2	50.3	51.5	37.6	38.5	41.1	40.6
Spessartine	14.8	1.3	13.5	4.8	16.2	11.7	11.8	12.4	14.5	7.9	30.6	32.3	43.2	45.2	35.6	36.0
Grossular	16.3	9.3	16.5	11.7	11.5	4.9	6.7	7.0	18.9	12.7	5.9	5.7	4.6	4.6	4.8	6.3

Spectrometer search shows < 0.2 wt % TiO_2 in any garnet.

of the host rocks. Although the sulfur in the analyses of the lower-grade black schists is very small (rocks 1153 and 1211, table 1), the high Mn contents of the garnets (table 6) in these rocks imply that sulfide was originally very abundant and has been removed by weathering.

The analyses show definite zoning of most of the garnets. In rock 135, small garnet euhedra have thin rims separated from interiors by rings of tiny inclusions (pl. 1). Rims of garnets in kyanite-bearing black schists are generally richer in Mn than the cores, in contrast to the zoning usually seen in garnets. In figure 5 and in geothermometric-geobarometric calculations, rim compositions are used. The zoning of garnet suggests that garnet participated in the isograd reactions producing staurolite and kyanite, if only to a limited degree.

Staurolite.—The compositions of analyzed staurolites (table 8) are close to the theoretical formula of $(Fe, Mg)_2Al_9Si_4O_{23}(OH)$. Small amounts of Ti and Mn are present. The Mg/(Mg + Fe) ratios cover a small range and are highest in the staurolites coexisting with kyanite in the few intermediate-color schists.

ZnO was analyzed by 5-min spectrometer counts at high beam current in some of the staurolites. Amounts were less than 0.2 wt percent in all samples.

Plagioclase.—Most of the mica schist plagioclase is oligoclase (table 9). Exceptions are An33 in staurolite-bearing schist 534 and An38 in kyanite–staurolite schist 1318. The garnet-zone plagioclases show remark-

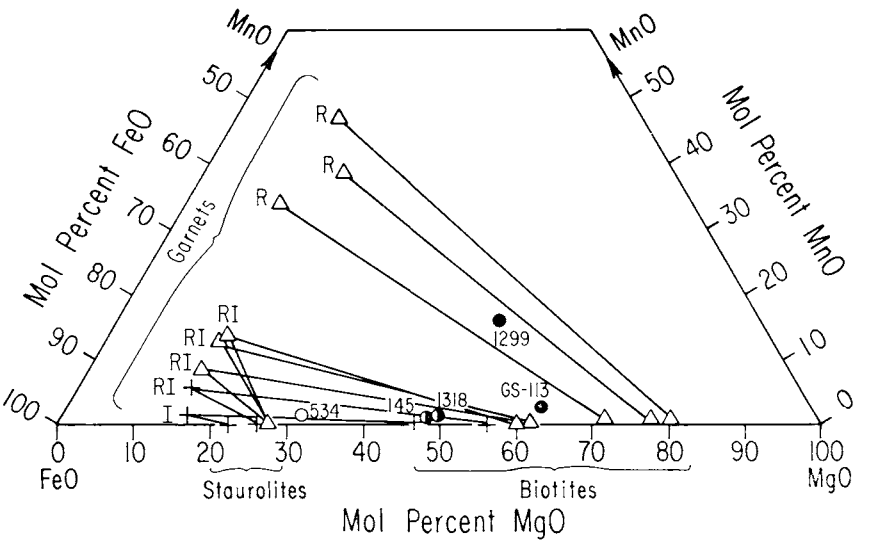

Fig. 5. Compositions of garnets, staurolites and biotites in the staurolite–kyanite zone. Triangles denote assemblages with kyanite. Crosses denote assemblages without kyanite. Tie-lines join coexisting phases. R denotes rutile present. I denotes ilmenite present. Circles show *effective* compositions in the subsystem FeO–MgO–MnO, after correction for FeS contents, of five rocks (see text). Filled circle indicates kyanite present, half-filled circle indicates kyanite and staurolite present, and open circle indicates staurolite present.

able inhomogeneity within individual grains, with analyses falling in two clusters in most cases, at An0-5 and An19-25. One low-grade sample, rock 1126, has relatively large plagioclase grains uniform at An10 which may be detrital relics. The variation in other low-grade samples may be due to an equilibrium peristerite gap or, following the earlier discussion about white mica compositions, may simply be due to failure of equilibration in a rising-temperature regime until a pervasive hydrous flux appeared as staurolite and kyanite formed at chlorite breakdown, at which time the plagioclase compositions jumped to near-equilibrium values.

A striking feature of some kyanite-grade black schists is large plagioclase porphyroblasts with broad inclusion-filled interiors of composition about An25 and thin, inclusion-free rims of plagioclase as sodic as An12 (pl. 1). The orientations of inclusions, mainly quartz and white mica, indicate rotation during growth, and this growth is probably part of a discontinuous kyanite-generating reaction. This increase in albite content of plagioclase with metamorphic grade contrasts with decrease in albite content of plagioclase in somewhat Ca-richer rocks (Wenk, 1962). Plagioclase and paragonite commonly coexist in kyanite-grade black schists, in contrast to the lower-grade black schists, and the sodic overgrowths of

TABLE 8
Staurolite analyses

	Gray Schists		Intermediate Schists		
Sample number	233	534	145	451	1318
Procedure used	EDS	EDS	EDS	EDS	EDS
Wt. % oxides					
MgO	2.49	2.58	2.58	2.66	2.66
Al_2O_3	54.84	54.29	55.63	54.54	54.60
SiO_2	27.96	28.38	28.49	28.51	28.45
CaO	0.00	0.00	0.00	0.00	0.00
TiO_2	0.58	0.60	0.69	0.45	0.49
MnO	0.00	0.00	0.00	0.00	0.00
FeO	14.18	13.48	12.75	13.02	12.77
Total oxide	100.05	99.33	100.14	99.18	98.98
Atoms/47 oxygens					
Si	3.88	3.95	3.92	3.97	3.96
Al	0.12	0.05	0.08	0.03	0.04
IV	4.00	4.00	4.00	4.00	4.00
Al	8.84	8.86	8.94	8.91	8.92
Ti	0.06	0.06	0.07	0.05	0.05
Mg	0.52	0.54	0.53	0.55	0.55
Mn	0.00	0.00	0.00	0.00	0.00
Fe	1.65	1.57	1.47	1.51	1.49
VI	11.07	11.03	11.01	11.02	11.01
Total Al	8.96	8.91	9.02	8.94	8.96
Mg+Fe	2.17	2.11	2.00	2.06	2.04
Mg/Mg+Fe	0.24	0.26	0.27	0.27	0.27

Spectrometer analyses of 233, 534 and 451 show < 0.3 wt % MnO or ZnO.

porphyroblasts may herald the approach of the paragonite–quartz stability limits. High-grade black schists containing paragonite and plagioclase are not systematically higher in CaO than lower-grade black schists containing paragonite without plagioclase.

Ilmenite.—All ilmenite is close to the ideal formula of $FeTiO_3$, with small amounts of Mg, Mn, and Al (table 10). Mn content correlates with the Mn levels of garnet rims. A slight decrease in Ti and increase in Fe + Mg occurs at the staurolite isograd; this may again be the effect of the elimination of low-grade metastability.

The appearance of ilmenite rather than rutile as the Ti oxide mineral in high-grade schists is closely related to biotite and garnet compositions, as shown in figure 5. FeO-rich (FeS-poor) bulk compositions yield ilmenite without rutile, FeO-poor (FeS-rich) compositions yield rutile without ilmenite, and intermediate compositions yield ilmenite + rutile.

Pyrrhotite.—All sulfides analyzed were pyrrhotite except for occasional pyrite or marcasite along cracks in, or as irregular patches in, pyrrhotite, which indicates that the FeS_2 is a secondary alteration and not a primary metamorphic mineral. Pyrrhotite probe analyses were $Fe_{0.85\pm0.02}S$ for both black and gray schists. By contrast, the X-ray diffraction data for the few black and intermediate schists from which pyrrhotite could be separated yielded a composition of $Fe_{0.91\pm0.01}S$. Ni and Co were sought with spectrometer analyses but were below the level of detection (0.05 wt percent). It is not clear why the two kinds of analysis gave different results. It is conceivable that low temperature secondary alteration produced uniform fine FeS_2 intergrowth in the pyrrhotites. As will be shown, the composition $Fe_{0.91}S$ is a thermodynamically plausible composition at the probable metamorphic conditions, whereas $Fe_{0.85}S$ is not.

Minor minerals.—In addition to the analyzed minerals, apatite, zircon and tourmaline were occasionally encountered in both gray and black schists. Rutile is the characteristic Ti mineral of the dark schists. Sphene occurs only in the quartz–chlorite rocks and is the only Ti mineral in

TABLE 9

Plagioclase compositions

Zone	Schist type	Sample	Ab Mol %	Variation
Garnet	Gray	1126	10	uniform
	Gray	1165	19-0	peristerite
	Black	1153	20-3	peristerite
Transition	Black	194	25-5	peristerite
	Black	212	25-5	peristerite
Staurolite–Kyanite	Gray	233	25	uniform
	Gray	534	33	uniform
	Inter.	145	24	uniform
	Inter.	451	25	uniform
	Inter.	1318	38	uniform
	Black	1299	22-14	normal zoning
	Black	GS-113	23-14	normal zoning
	Black	135	23-16	normal zoning

Or mol percent nearly constant at 0.5.

TABLE 10
Ilmenite analyses

	GARNET ZONE		STAUROLITE ZONE				
	Gray Schists		Gray Schists		Intermediate Schists		
	1126	1165	233	534	1318	451	145
MgO	0.43	0.28	0.60	0.68	0.99	0.90	0.20
Al_2O_3	0.60	0.64	0.57	0.56	0.55	0.50	0.64
TiO_2	53.13	53.08	51.33	51.69	51.89	53.07	52.44
MnO	0.71	1.29	0.00	0.05	0.93	0.77	0.96
FeO	44.33	44.20	47.37	47.10	46.11	44.45	44.81
Total oxide	99.20	99.49	99.87	100.08	100.47	99.69	99.02
Atoms/6 oxygens							
Ti	1.983	1.983	1.929	1.938	1.932	1.965	1.978
Al	0.035	0.037	0.034	0.033	0.032	0.029	0.038
Mg	0.036	0.021	0.044	0.050	0.072	0.065	0.015
Mn	0.030	0.055	0.000	0.002	0.039	0.077	0.041
Fe	1.840	1.837	1.980	1.963	1.909	1.831	1.882
Mg+Mn+Fe	1.906	1.913	2.024	2.015	2.020	1.928	1.976

these rocks. This fact, and the presence of apatite and Ca-rich garnet, may be evidence of a meta-carbonate origin of the quartz–chlorite pods.

CONDITIONS OF METAMORPHISM

Compositional control.—The effective Mg/(Mg + Fe) ratio was a prime determinant of the metamorphic assemblages. This quantity may be estimated from the sulfur analyses of table 2 for the little-weathered high-grade specimens. The apparent average pyrrhotite composition from microprobe analysis is $Fe_{0.85}S$. If a pyrrhotite equivalent of Fe is subtracted from the spectroscopic FeO value of table 2, the remaining iron gives the effective ratio $Fe^{2+}/(Fe^{2+} + Mg + Mn)$, assuming that no Fe is trivalent. Figure 5 shows the effective molar fractions of Mg, Mn, and Fe for the staurolite–kyanite grade rocks. The rocks with effective Fe fraction less than 0.4 have kyanite but no staurolite. Rocks in the range about 0.5 have staurolite and kyanite, and rocks in the range above 0.65 have staurolite but no kyanite. Control by the effective bulk composition over the appearance of rutile and ilmenite and of the garnet compositions is also evident. Four key assemblages can be recognized as indicators of progressive sulfur activity and iron depletion, analogous to the seven assemblages recognized for sillimanite-grade rocks by Robinson and Tracy (1977): (1) staurolite–ilmenite, (2) staurolite–ilmenite–rutile, (3) kyanite–staurolite–ilmenite–rutile, and (4) kyanite–rutile. It is probable that additional assemblages between (3) and (4) could eventually be found. It must be emphasized, however, that the gray and black schists are somewhat discrete entities, and that rocks transitional between them are rare.

Temperatures and pressures of metamorphism.—The physical conditions of metamorphism can be estimated from quantitative geothermometry-geobarometry based on mineral solid solutions or, within temperature and pressure limits, by bounding experimental univariant phase equilibrium curves. The use of experimental dehydration equilibria depends on the assumption that P_{H_2O} was a large fraction of P_{total}. Although, as will be shown, P_{H_2O} cannot be calculated accurately from the schist assemblages, very similar assemblages in slightly more CaO-rich rocks in the Ducktown area contain the additional phases sphene and calcite, enabling a more exact calculation. From this information and the presence of ubiquitous calc–silicate pods, Nesbitt (ms) calculated that P_{H_2O} averaged about 85 percent of P_{total}. The assemblage clinozoisite–plagioclase is common in calc–silicate pods of the Anakeesta rocks, which suggests that P_{H_2O} is a large fraction of P_{total}. If $P_{H_2O} = 0.85P_{total}$, it can be shown that the dehydration curves are lowered only a few degrees below their experimental positions for $P_{H_2O} = P_{total}$. For this reason, and because they serve only as extreme temperature limits, the dehydration curves used here are taken unmodified from the experimental data.

The experimental curve for the reaction of chlorite + muscovite to staurolite + biotite + quartz + vapor (Hoschek, 1969) is an important indicator. This reaction curve shown in figure 6 is not truly univariant in the system K_2O–FeO–MgO–Al_2O_3–SiO_2–H_2O, but represents the trace of a divariant surface for a fixed Mg/(Mg + Fe) ratio of 0.4 in Hoschek's

experimental system. This corresponds fairly closely to the Mg-values of rocks 1126 and 1165, which are garnet-zone gray schists with primary chlorite. Figure 6 also shows the experimental reaction curves of paragonite + quartz to albite + Al_2SiO_5 + vapor (Chatterjee, 1972), which serves as an upper temperature limit for the Anakeesta schists, because paragonite and quartz are stable to the highest grade attained by the metamorphism. The granite melting minimum also gives effective upper temperature limits (fig. 6).

Garnet–biotite K_D geothermometry based on experimental Fe–Mg distributions (Ferry and Spear, 1978) or semi-empirical constructions (Perchuk, Podlesskii, and Aranovich, 1981) has dubious application to most of the Anakeesta rocks because of the anomalous compositions of the minerals, which depart widely from experimental or model systems. Staurolite-bearing rocks with the lowest Ca + Mn in garnets and biotites of the smallest alkali deficiencies, namely rocks 233 and 534, were used for biotite–garnet thermometry. At a representative pressure of 6 kb, the Ferry-Spear thermometer gave 511° to 514°C and the Perchuk, Podlesskii, and Aranovich thermometer gave 523° to 527°C. These temperatures are considerably lower than the minimum estimates afforded by the experimental staurolite-forming curve of Hoschek (1969) and are regarded only as absolute lower limits. White mica solvus thermometry based on the Eugster and others (1972) experiments gives, as discussed earlier, probable temperature overestimates near 600°C. Because of the limitations of these geothermometers, only broad temperature estimates can be set between the univariant equilibrium curves. The temperature estimate

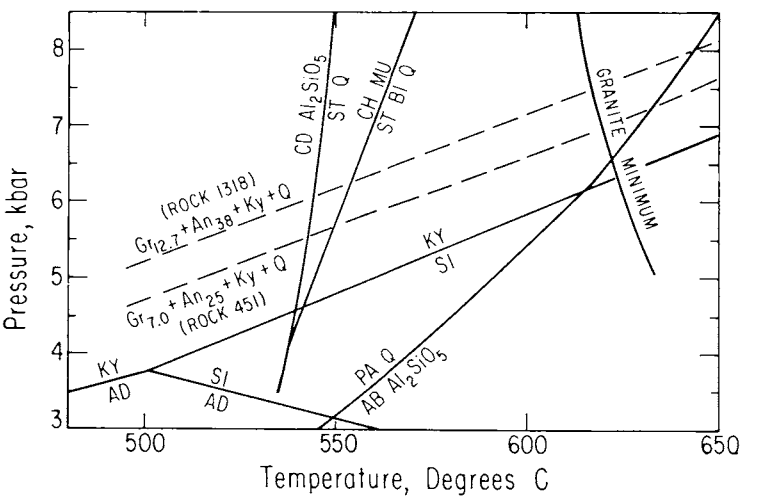

Fig. 6. Experimental univariant equilibria bearing on calculated pressures and temperatures of kyanite–staurolite metamorphism and P–T lines of constant mineral compositions for two rocks. See text for sources. CD denotes chloritoid, ST staurolite, KY kyanite, SI sillimanite, AD andalusite, PA paragonite, AB albite, CH chlorite, MU muscovite, BI biotite, and Q quartz. Gr and An denote $Ca_3Al_2Si_3O_{12}$ mol fraction of garnet and $CaAl_2Si_2O_8$ mol fraction of plagioclase, respectively.

yielded by figure 6 centers at about 580°C with as much as ± 35°C uncertainty.

The garnet–plagioclase–Al_2SiO_5–quartz geobarometer is applicable to those Anakeesta schists containing the four-phase assemblage in which the Mn contents of the garnets are small. This criterion limits the selection to staurolite–kyanite rocks 451 and 1318. The field calibration of Ghent, Robbins, and Stout (1979) is accepted, because it was constructed from kyanite-bearing assemblages in the same general temperature range of the Anakeesta rocks and because it has been shown to agree with boundary conditions set by measured thermodynamic properties of grossular (Newton and Haselton, 1981). The Ghent, Robbins, and Stout barometric equation is:

$$\log\left(\frac{X_{gr}^{gt}}{X_{an}^{pl}}\right)^3 - \frac{1}{T}(0.3448P + 3272) + 7.9969 = 0 \qquad (1)$$

The original equation as given by Ghent, Robbins, and Stout (1979, p. 878) involved a factor of 3448, rather than 0.3448, due to a missprint. In this equation, X_{gr}^{gt} denotes the grossular mol fraction of garnet and X_{an}^{pl} the anorthite mol fraction of the coexisting plagioclase. Pressure is in bars and temperature in Kelvins. The P-T curves based on eq (1) for rocks 451 and 1318 are shown in figure 6. Assuming that the pressure band defined by them is representative, the maximum pressure spread for the kyanite–staurolite zone Anakeesta rocks is 5.7 to 7.5 kb, depending on temperature in the range 545° to 615°C defined by the Hoschek (1969) staurolite-forming line and the granite minimum. These P-T estimates are compatible with the experimental lower-temperature stability limits for staurolite–quartz (Hoschek, 1967; Richardson, 1968), with the upper-temperature limit for paragonite–quartz (Chatterjee, 1972), and the experimental Al_2SiO_5 polymorph stability relations (Holdaway, 1971), as shown in figure 6.

The P-T estimates of 6.6 ± 0.9 kb and 580°C ± 35°C inferred for the Anakeesta rocks are similar to those estimated by Nesbitt and Essene (1982) for the nearly isofacial Ocoee rocks of the Ducktown area. They deduced 6.0 ± 1.0 kb and 540° ± 30°C based on calcite–dolomite thermometry, oxygen isotope thermometry, and many experimental univariant equilibria of calc–silicate minerals present in that area, as well as from garnet–plagioclase–kyanite–quartz barometry.

Metamorphic fluids.—Thermodynamic data for minerals occurring in the Anakeesta schists are insufficient at present to allow precise calculation of the fluid compositions coexisting with them at the height of metamorphism. Definitive minerals present in the Ducktown area, such as magnetite, sphene, and calcite, are very rare or absent in the Anakeesta rocks. Although the major Fe-bearing silicates, together with graphite, oxides, and sulfides, controlled the fluid compositions, free energy of formation and activity data are not available for the Fe components of garnet, biotite, or staurolite. This is especially true for the Mn-rich garnets and peraluminous, K-deficient biotites of the Anakeesta Formation. Al-

though mixing parameters could be estimated from various crystallographic models for silicate minerals, such estimates are highly uncertain.

In principle, the assemblage ilmenite (il)–rutile (ru)–graphite (gr)–pyrrhotite (po) defines the vapor phase in the system C–O–H–S coexisting with it at any pressure and temperature, and there are measured thermodynamic data for these substances. In practice, the uncertainties in the data do not permit very precise calculations, and the observed pyrrhotite composition, a key parameter, may not be representative of the peak metamorphic conditions due to subsequent changes (Craig and Scott, 1974). Nevertheless, a calculation of vapor compositions which could have coexisted with the observed Anakeesta pyrrhotites and the other minerals proves instructive.

The reactions governing the vapor composition are:

$$C(gr) + O_2 = CO_2 \qquad (D)$$

$$2C(gr) + 2H_2O = CO_2 + CH_4 \qquad (E)$$

$$2FeTiO_3(il) + S_2 = 2FeS(po) + 2TiO_2(ru) + O_2 \qquad (F)$$

The assumption is made, following Eugster and Skippen (1967) and Ohmoto and Kerrick (1977), that H_2, CO, hydrocarbons, and sulfur-bearing species are quantitatively negligible in the vapor phase. There are thus three equilibrium conditions:

$$K_C = \frac{f_{CO_2}}{f_{O_2}}$$

$$K_D = \frac{f_{CO_2} \cdot f_{CH_4}}{f_{H_2O}^2} \qquad (2)$$

$$K_E = \frac{f_{O_2} \cdot (\alpha_{FeS}{}^{po})^2}{f_{S_2}}$$

where f denotes fugacity, α activity, and the K's are constants at constant T and P, from which to determine the four unknown quantities P_{H_2O}, P_{CO_2}, P_{O_2}, and P_{CH_4}. A fourth equation needed is the assumption that the sum of the partial pressures (essentially $P_{H_2O} + P_{CO_2} + P_{CH_4}$) equals the total pressure. The quantities $\alpha_{FeS}{}^{po}$ and f_{S_2} are determined by the pyrrhotite composition at any T and P through the experimental work of Toulmin and Barton (1964). Since that work was done at confining pressures of nearly zero (Barton and Toulmin, 1964), the equilibrium constants, f_{S_2} and $\alpha_{FeS}{}^{po}$, have to be corrected by a solid volume compression to 7000 bars, the assumed pressure of the equilibration. In practice, the correction for $\alpha_{FeS}{}^{po}$ is negligible (Craig and Scott, 1974), but that for f_{S_2} is not. Toulmin and Barton's (1964) estimated partial molar volume of S_2 in pyrrhotite of 16.2 cm^3 was used in this calculation. The other necessary quantities, free energies of formation and molar volumes of the solids, were taken from Robie, Hemingway, and Fisher (1978).

Figure 7 shows isobars of CO_2 plotted as functions of temperature and pyrrhotite composition. The f_{CO_2} values from the preceding calcula-

tion were converted to pressures with the fugacity coefficients of Burnham and Wall (unpub.), and the assumption of Lewis-Randall (ideal) gas mixing was used. Figure 7 shows that at any allowed partial pressure of CO_2, pyrrhotite in equilibrium with rutile, ilmenite, graphite, and the vapor phase becomes enriched in iron as temperature rises. The more sulfur-rich compositions of pyrrhotite are not allowed, because partial pressure of CO_2 may not exceed total pressure.

Figure 7 shows that the range of pyrrhotite compositions determined by X-ray diffraction are consistent with measured thermodynamic data under the assumption that these compositions represent the peak metamorphic conditions. The constant value for N_{FeS} of 0.953 implies a preponderance of the $Fe_{10}S_{11}$ phase, which is stable at low temperature (Craig and Scott, 1974). In order for the pyrrhotite composition to have changed substantially during cooling from peak metamorphic temperatures there would have to have been extensive interactions with silicate and oxide phases; such a requirement may have limited the back-reaction. The considerably more sulfur-rich compositions given by the microprobe analyses are not allowed at peak metamorphic conditions by the thermodynamic data, since they would require impossibly high CO_2 pressures as well as primary pyrite, which is not observed. The microprobe analyses may be

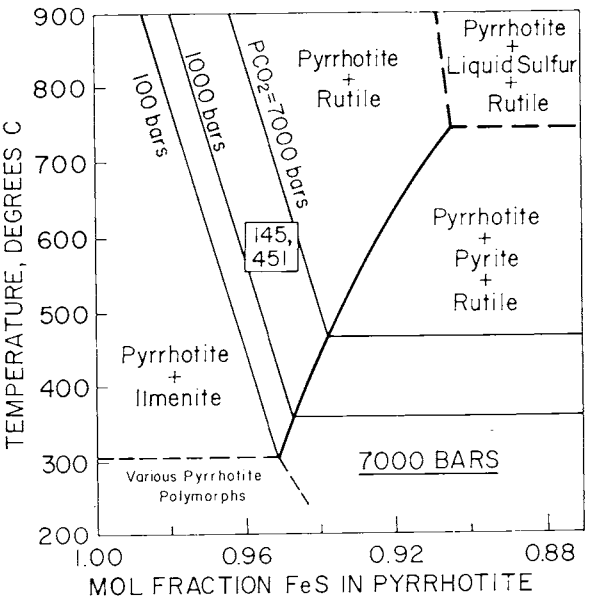

Fig. 7. Dependence of pyrrhotite composition in the system FeS–S_2 on temperature at 7000 bars total pressure, for coexisting pyrrhotite, ilmenite, rutile, and vapor. Isobars of CO_2 superposed. The composition of pyrrhotite in rocks 145 and 451, containing the three-mineral assemblage, is shown as determined by X-ray diffraction. This diagram shows that the presently observed composition is consistent with both the allowable range of CO_2 pressures at the deduced P and T conditions of metamorphism, and with exsolution of a small amount of pyrite from pyrrhotite compositions originally slightly more sulfur-rich.

affected by very fine-grained and pervasive pyrite or marcasite alteration of supergene origin. The thermodynamic data are compatible with change of pyrrhotite composition during cooling by the exsolution of a small amount of pyrite, and the pyrrhotite may have been slightly more sulfur-rich than deduced by X-ray diffraction.

PETROLOGIC INTERPRETATION

A number of the mineralogic peculiarities of the Anakeesta rocks are also displayed in other sulfidic-graphitic metamorphic rocks and therefore may be traceable to the presence of abundant sulfur and carbon. Some of these features are directly attributable to silicate iron depletion, such as the great spread of biotite Mg/(Mg + Fe) ratios and the high Mn levels of garnets. Other features, such as the low alkali contents of some biotites, the paragonite–plagioclase "isograd" in black schists, the Na-rich high-grade overgrowths on plagioclase, and the increase in Mn contents of garnet rims in high grade black schists, may possibly be indirectly attributed to the presence of abundant sulfide and graphite. These interpretations are, necessarily, very conjectural and are offered here merely to emphasize the probability of more subtle, far-reaching effects of iron depletion, affecting, ultimately, the non-ferromagnesian minerals.

Isograd reactions.—Figures 8 and 9 show Thompson AFM projections for mica schists of garnet and staurolite–kyanite zone, respectively, to illustrate mineralogic reactions generating the isograds. Abundant staurolite appears abruptly in the gray schists. Matrix chlorite disappears completely over no more than 0.5 km normal to the isograd trace. These features indicate a reaction of the sort envisioned by Albee (1965) and Ghent (1975):

chlorite + muscovite + garnet = staurolite + biotite + quartz + vapor (G)

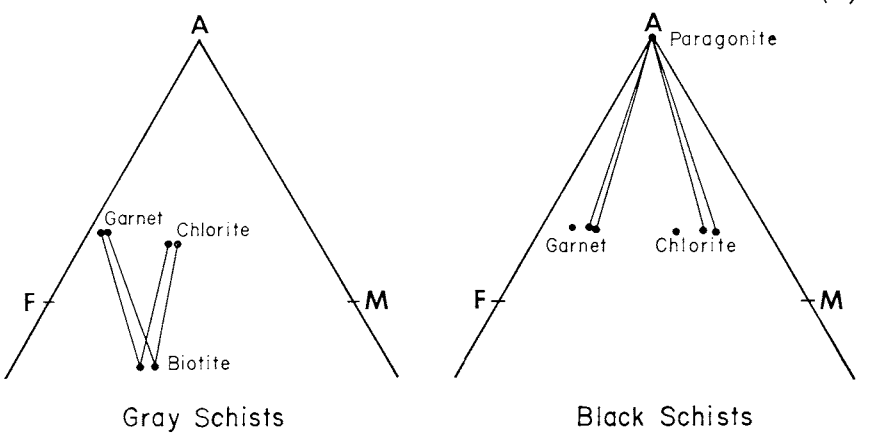

Fig. 8. AFM plots of garnet-grade gray and black schists. Garnet–chlorite tie lines are removed for clarity. Gray schists contain biotite; black schists with very high Mg/(Fe + Mg) ratios contain paragonite. A trend toward more aluminous compositions with increase in Mg/(Fe + Mg) ratio is apparent.

which is univariant in the system K_2O–FeO–MgO–Al_2O_3–SiO_2–H_2O. Small amounts of other components, such as MnO in garnet and TiO_2 in biotite, will not increase the variance significantly; this probably accounts for the sharpness of the isogradic trace.

Staurolite is found in non-sulfidic, oxidized schists in the map area of figure 1 west of the isogradic trace in the Anakeesta Formation, and Carpenter's (1970) regional staurolite isograd passes several kilometers west of the Anakeesta staurolite isograd. It is conceivable that staurolite appearance in pelites of high oxygen fugacity and/or greater effective FeO content occurs as a higher-variance reaction which begins at a lower temperature than that prevailing during the Anakeesta isograd reaction. Under this interpretation, the staurolite isograd is deferred to higher grade, principally because of the relatively refractory Mg-rich chlorite involved, until a sufficiently high grade corresponding to the near-univariant reaction (G). An alternative hypothesis is that a local depression of the isogradic surface is present within the area studied. Such depressions are known within the Murphy syncline east of the Ducktown region (Nesbitt and Essene, 1982). Carpenter's (1970) regional isograds were determined by reconnaissance survey and may eventually be somewhat modified in detail.

Kyanite appears more gradually in the Anakeesta rocks, over a zone of nearly 2 km. Since garnets are stabilized by their Mn contents, their presence does not require a univariant reaction. More likely the reaction is at least divariant:

$$\text{chlorite} + \text{muscovite} = \text{kyanite} + \text{biotite} + \text{quartz} + \text{vapor} \qquad \text{(H)}$$

Approximate experimental determinations of the Fe-free reaction (H) by Seifert (1970) and Bird and Fawcett (1973) place it near 650°C at 6 kb.

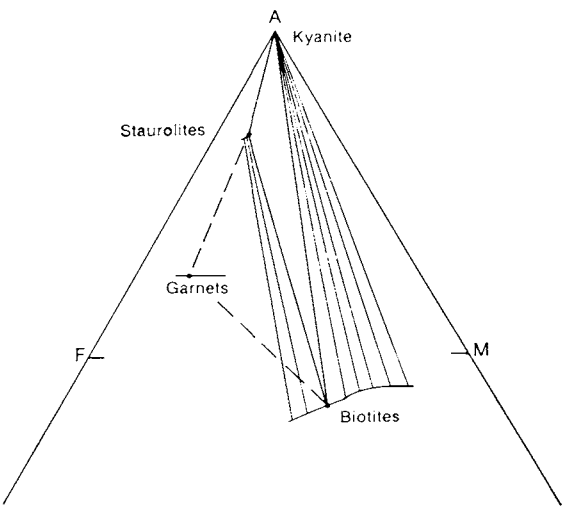

Fig. 9. AFM plot of kyanite–staurolite grade schists. Assemblages staurolite–biotite, staurolite–kyanite–biotite, and kyanite–biotite occur. All schists contain garnet also, but garnet is inconsistent with the AFM plot for most rocks, being stabilized by Mn.

This temperature is considerably higher than deduced earlier for the staurolite–kyanite zone Anakeesta rocks, which indicates that Fe depletion is not so pronounced as in some very sulfur-rich rocks, such as the Small's Falls Formation (Guidotti, Cheney, and Conatore, 1975a), where chlorite is stabilized to its absolute upper stability limit.

The role of quartz–chlorite rocks.—The replacement of chlorite by biotite in the quartz–chlorite rocks near the kyanite isograd requires substantial migration of K_2O within the black schist units. Also, amounts of chlorite present within the mica schists themselves seem inadequate to have accounted for the large amounts of kyanite found in some of the higher-grade rocks. It is possible that equilibrium with respect to the chemical potential of K_2O was achieved over a distance of a few meters, leading to reaction between muscovite of the black mica schists and chlorite of the quartz–chlorite pods. The quartz–chlorite pods thus may have acted as a sink for potassium at a certain stage in the metamorphism, which effectively promoted kyanite development.

Paragonite–plagioclase isograd.—Inspection of figure 2 shows that a substantial enrichment of Na_2O in muscovite occurs across the kyanite isograd. This enrichment is probably residual and is due to separation of K_2O from muscovite to form biotite. In cases where the soda content of muscovite was already high and where considerable amounts of chlorite were available for reaction, this enrichment was sufficient to cause formation of paragonite as a separate phase. It is likely that paragonite first appears as a discrete phase in a number of beds at the kyanite isograd.

Some, and in many cases all, of this paragonite subsequently reacted to form plagioclase porphyroblasts. The unzoned oligoclase cores of these porphyroblasts imply that CaO was furnished by breakdown of another discrete phase. No suitable CaO-bearing phases were identified in black mica schists of the garnet zone. Possibly small amounts of matrix calcite were present within the garnet zone and were consumed by the reaction. The lack of calcite in low-grade black schists could result from weathering. Slight increases in CaO content of analyzed rocks across the isograds are compatible with this hypothesis. Because of uncertainty as to the source of CaO, specific reactions for formation of plagioclase cores cannot be written. The abundant quartz inclusions within the oligoclase cores suggest that quartz was not a reactant.

Anomalous plagioclase zoning.—Normally-zoned rims on plagioclase porphyroblasts can be explained by the simple reaction studied by Chatterjee (1972);

$$\text{paragonite} + \text{quartz} = \text{albite} + \text{kyanite} + \text{vapor} \qquad \text{(I)}$$

Coexistence of paragonite, plagioclase, kyanite, and quartz to the highest grades studied indicates that temperatures remained below those required for reaction of the pure phases. The fact that these zoned rims contain few quartz inclusions suggests that quartz was a reactant, as required by the proposed reaction, which further implies that the character of the

plagioclase-forming reaction changed when the unknown source of CaO failed.

Anomalous biotite compositions.—The low alkali contents of biotites from the darkest schists appear to be a primary feature, rather than one due to retrogressive alteration. A possible explanation is that biotite and refractory Mg–chlorite may form mixed-layer phases at a certain metamorphic grade in aluminous rocks. Detailed crystallo-chemical studies are needed to substantiate this hypothesis. Seifert (1970) reported a possible occurrence of a mixed biotite–chlorite during experimental work on the system K_2O–MgO–Al_2O_3–SiO_2–H_2O. Bird and Fawcett (1973) looked for, but did not find, such a phase.

Complex substitutions within the crystal structure of biotite may also explain the decrease of K_2O content with increase in the Mg/(Fe + Mg) ratio. Decrease in K, Ti, and to a very slight extent Al are balanced by increase in Si, total Fe + Mg + Mn, and by increase in occupancy of the octahedral site.

Control of Ti-oxide minerals.—The presence of ilmenite or rutile is dictated by the effective FeO contents, as shown in figure 5. Rutile pseudomorphs after ilmenite in a few black schists may be evidence for some continuous depletion of iron from the silicates by pyrrhotite with increasing grade.

Anomalous Mn-zoning of garnet.—Garnet is stabilized against drastic Fe-depletion in the most sulfur-rich schists by high Mn-content and would not otherwise appear in the kyanite-bearing schists, as shown in the AFM diagram of figure 9. Garnets of the high-grade black schists have slightly but definitely more Mn-rich rims. This indicates that progressive biotite growth absorbs iron from the other ferromagnesian silicates and the garnet "hangs on" only by virtue of increased Mn content.

General trends of sulfide metamorphism.—Within the Anakeesta Formation, sulfur is probably of syngenetic origin. Pre-orogenic igneous rocks within the entire Great Smoky Group are limited to sparse, widely separated diabase dikes and sills (Hadley and Goldsmith, 1963; Hurst, 1955); none were found within the area studied here. Distribution of sulfide within the Anakeesta Formation is controlled entirely by the stratigraphy, even on outcrop scale. A near-exact correlation exists between amounts of sulfur and carbon for all analyzed mica schists that have not been subject to weathering (fig. 10). The favored model is that of Berner (1970), in which bacterial reduction of $SO_4^=$ ions in seawater with utilization of organic carbon leads eventually to formation of pyrite and depletion of iron from non-sulfide minerals.

Further iron-depletion of oxide and silicate phases probably occurs at the pyrrhotite isograd (Carpenter, 1974) by the general reaction:

$$\text{pyrite} + \text{Fe-silicates} + \text{carbon} = \text{pyrrhotite} + \text{Fe-poorer silicates} + CO_2$$

Reduction of sulfur is balanced by oxidation of carbon. Presence of graphite and iron-bearing silicates result in low fugacity values for both oxygen and sulfur and in low partial pressures of all sulfur-bearing gases (Froese, 1977; Nesbitt, ms). On the other hand, a substantial partial pres-

sure of CO_2 is generated. The overall result is a decrease in graphite content of the pelitic rocks, while sulfur content remains essentially unchanged. The high ratio of sulfur to carbon within mica schists of the Anakeesta Formation (fig. 10), well beyond the envelope for modern marine clays and shales (Goldhaber and Kaplan, 1975), may indicate that much original condensed carbon is lost to a vapor phase in metamorphism.

Within graphitic mica schists, pyrrhotite may become more iron-rich with increasing metamorphic grade. Such a trend is evident for the assemblage ilmenite–rutile–graphite–pyrrhotite (fig. 7) and may also apply to equilibria between silicate minerals and pyrrhotite. An increase of iron-content of pyrrhotite with grade is suggested by the observation of Carpenter (1974) that monoclinic pyrrhotite is the abundant polymorph of the biotite zone, whereas higher-grade pelites generally contain hexagonal pyrrhotite. Iron-depletion of non-sulfide phases with grade is suggested by rutile pseudomorphs after ilmenite within garnet-zone black mica schists whose silicate Mg/(Fe + Mg) ratios are moderate, by the first appearance of rutile within transitional and certain gray mica schists of the staurolite–kyanite zone, and by increase of Mn contents of rims of zoned black schist garnets.

The overall effect of sulfur on metamorphism of the Anakeesta Formation is therefore profound, even though none of the proposed silicate reactions involves pyrrhotite as an essential phase. Low-sulfur fugacities and partial pressures of any sulfur-bearing gas species greatly inhibit diffusion of sulfur and effectively maintain separate systems within the various strata studied (Thompson, 1972). This is true for metamorphic temperatures of middle-amphibolite grade locally and also for higher

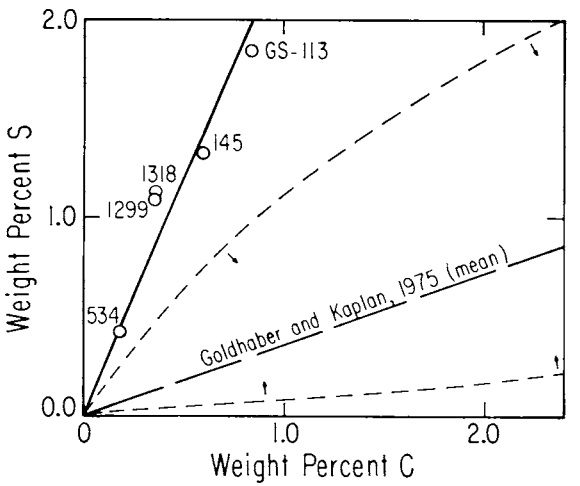

Fig. 10. Correlation of S and C in least-weathered schists. Average S–C correlation of Goldhaber and Kaplan (1975) for young marine sediments is indicated, and the envelope for all analytic data given by them is shown by dashes and arrows. The highly correlated S and C contents projecting through the origin is evidence for a sedimentary-diagenetic origin of the C and S contents.

grades elsewhere (Robinson and Tracy, 1977). Within each unit of graphite-bearing rock, fugacity of sulfur during metamorphism and oxide and silicate phases present at equilibrium are dependent mainly on the initial composition of the parent shale, especially on its initial sulfide content, as well as on pressure and temperature of metamorphism.

ACKNOWLEDGMENTS

The field work of this study and some of the microprobe analyses were supported by an NSF grant, #GA 22904 (RCN). Rock analyses and additional mineral analyses were supported by NSF EAR 78-15939 (RCN). Microprobe analyses at the University of Western Ontario were supported by the McMaster University Science and Engineering Research Board, through research grant #214-7397-000. We are grateful to R. A. Barnett for these analyses, to the Department of Geosciences, Virginia Polytechnic Institute and State University, for use of their microprobe, to D. W. Rankin of the U.S. Geological Survey and A. T. Anderson of the Department of the Geophysical Sciences at the University of Chicago for valuable guidance in the field work, and to R. C. Aller, also at Chicago, for discussions on shale diagenesis. We also wish to acknowledge constructive criticisms of the original manuscript of this paper by Bruce Nesbitt and Robert J. Tracy.

REFERENCES

Albee, A. L., 1965, A petrogenetic grid for the Fe–Mg silicates of pelitic schists: Am. Jour. Sci., v. 263, p. 512-536.

Bachinski, D. J., 1976, Metamorphism of cupiferous iron sulfide deposits, Notre Dame Bay, Newfoundland: Econ. Geology, v. 71, p. 443-452.

Barton, P. B., and Toulmin, P. III, 1964, The electrum-tarnish method for the determination of the fugacity of sulfur in laboratory sulfide systems: Geochim. et Cosmochim. Acta, v. 28, p. 619-640.

Berner, R. A., 1970, Sedimentary pyrite formation: Am. Jour. Sci., v. 268, p. 1-23.

Bird, G. W., and Fawcett, J. J., 1973, Stability relations of Mg–chlorite–muscovite and quartz between 5 and 10 kb water pressure: Jour. Petrology, v. 14, p. 415-428.

Butler, J. R., 1972, Age of Paleozoic regional metamorphism in the Carolinas, Georgia, and Tennessee Southern Appalachians: Am. Jour. Sci., v. 272, p. 319-333.

Carpenter, R. A., 1970, Metamorphic history of the Blue Ridge Province of Tennessee and North Carolina: Geol. Soc. America Bull., v. 81, p. 749-762.

———— 1974, Pyrrhotite isograd in southeastern Tennessee and southwestern North Carolina: Geol. Soc. America Bull., v. 85, p. 451-456.

Chatterjee, N. D., 1972, The upper stability limit of the assemblage paragonite + quartz and its natural occurrence: Contr. Mineralogy Petrology, v. 34, p. 288-303.

Clark, D. A., 1969, Sulfurization of cordierite, Minas de Panasqueira, Portugal: Geol. Soc. Finland Bull., v. 41, p. 231-234.

Craig, J. R., and Scott, S. D., 1974, Sulfide phase equilibria: Min. Soc. America Short Course Notes, v. 1, p. CS-1 to CS-110.

Eugster, H. P., Albee, A. L., Blencoe, A. E., Thompson, J. B., and Waldbaum, D. R., 1972, The two-phase region and excess mixing properties of paragonite–muscovite crystalline solutions: Jour. Petrology, v. 13, p. 147-179.

Eugster, H. P., and Skippen, G. B., 1967, Igneous and metamorphic reactions involving gas equilibria, *in* Abelson, P. H., ed., Researches in Geochemistry, v. 2: New York, John Wiley & Sons, Inc., p. 492-520.

Ferry, J. M., and Spear, F. S., 1978, Experimental calibration of the partitioning of Fe and Mg between biotite and garnet: Contr. Mineralogy Petrology, v. 66, p. 113-117.

French, B. M., 1968, Progressive contact-metamorphism of the Biwabek iron-formation, Mesabi Range, Minnesota: Minnesota Geol. Survey Bull., v. 45, 103 p.

Frey, M., 1978, Progressive low-grade metamorphism of a black shale formation, Central Swiss Alps, with special reference to pyrophyllite and margarite bearing assemblages: Jour. Petrology, v. 19, p. 95-135.

Froese, E., 1971, The graphical representation of sulfide–silicate phase equilibria: Econ. Geology, v. 66, p. 335-341.

———— 1977, Oxidation and sulphidation reactions, *in* Greenwood, H. J., ed., Short Course in Application of Thermodynamics to Petrology and Ore Deposits: Mineralog. Assoc. Canada, Short Course Handbook, v. 2, p. 84-98.

Froese, E., and Gasparrini, E., 1975, Metamorphic zones in the Snow Lake Area, Manitoba: Canadian Mineralogist, v. 13, p. 162-167.

Ghent, E. D., 1975, Temperature, pressure, and mixed-volatile equilibria attending metamorphism of staurolite–kyanite bearing assemblages, Esplanade Range, British Columbia: Geol. Soc. America Bull., v. 86, p. 1654-1660.

Ghent, E. D., Robbins, D. B., and Stout, M. Z., 1979, Geothermometry, geobarometry, and fluid compositions of metamorphosed calc–silicates and pelites, Mica Creek, British Columbia: Am. Mineralogist, v. 64, p. 874-885.

Goldhaber, M. B., and Kaplan, I. R., 1975, Controls and consequences of sulfate reduction rates in recent marine sediments: Soil Sci., v. 119, p. 42-55.

Guidotti, C. V., 1970, The mineralogy and petrology of the transition from the lower to upper sillimanite zone in the Oquossoc area, Maine: Jour. Petrology, v. 11, p. 277-336.

———— 1974, Transition from staurolite to sillimanite zone, Rangeley Quadrangle, Maine: Geol. Soc. America Bull., v. 85, p. 475-490.

Guidotti, C. V., Cheney, J. T., and Conatore, P. D., 1975a, Coexisting cordierite + biotite + chlorite from the Rumford quadrangle, Maine: Geology, v. 4, p. 147-148.

———— 1975b, Interrelationship between Mg/Fe ratio and octahedral Al content in biotite: Am. Mineralogist, v. 60, p. 849-853.

Hadley, J. B., and Goldsmith, R., 1963, Geology of the eastern Great Smoky Mountains, North Carolina and Tennessee: U.S. Geol. Survey Prof. Paper 349-B, 118 p.

Hatcher, R. D., 1978, Tectonics of the western Piedmont and Blue Ridge, southern Appalachians: Review and speculation: Am. Jour. Sci., v. 278, p. 276-304.

Holdaway, M. J., 1971, Stability of andalusite and the aluminum silicate phase diagram: Am. Jour. Sci., v. 271, p. 97-131.

Holland, H. D., 1959, Some applications of thermochemical data to problems of ore deposits. I. Stability relations among the oxides, sulfides, sulfates, and carbonates of ore and gangue metals: Econ. Geology, v. 54, p. 184-233.

———— 1965, Some applications of thermochemical data to problems of ore deposits. II. Mineral assemblages and the composition of ore-forming fluids: Econ. Geology, v. 60, p. 1101-1166.

Hoschek, G., 1967, Untersuchungen zum Stabilitätsbereich von Chloritoid und Staurolith: Contr. Mineralogy Petrology, v. 14, p. 123-162.

———— 1969, The stability of staurolite and chloritoid and their significance in metamorphism of pelitic rocks: Contr. Mineralogy Petrology, v. 22, p. 207-232.

Hurst, V. J., 1955, Stratigraphy, structure, and mineral resources of the Mineral Bluff quadrangle, Georgia: Georgia Geol. Survey Bull. 63, 137 p.

Hutcheon, I., 1979, Sulfide–oxide–silicate equilibria, Snow Lake, Manitoba: Am. Jour. Sci., v. 279, p. 643-665.

Itaya, T., and Banno, S., 1980, Paragenesis of titanium-bearing accessories in the pelitic schists of the Sanbagawa belt, Central Shikoku, Japan: Contr. Mineralogy Petrology, v. 73, p. 267-276.

Keith, A., 1913, Production of apparent diorite by metamorphism: Geol. Soc. America Bull., v. 24, p. 684-685.

Marmo, V., and Mikkola, A., 1951, On sulphides of the sulphide-bearing schists of Finland: Comm. géol. Finlande Bull., v. 156, p. 5-55.

Miyashiro, A., 1973, Metamorphism and Metamorphic Belts: Boston, Allen and Unwin, 492 p.

Mohr, D. W., 1973, Stratigraphy and structure of part of the Great Smoky and Murphy belt groups, western North Carolina: Am. Jour. Sci., v. 273-A, p. 41-71.

Nesbitt, B. E., ms, 1979, Regional metamorphism of the Ducktown, Tennessee massive sulfides and adjoining portions of the southern Blue Ridge Province: Ph.D. dissert., The Univ. of Michigan, Ann Arbor, Mich., 238 p.

Nesbitt, B. E., and Essene, E. J., 1982, Metamorphic thermometry and barometry of a portion of the Southern Blue Ridge Province: Am. Jour. Sci., v. 282, p. 701-729.

Nesbitt, B. E., and Kelly, W. C., 1980, Metamorphic zonation of sulfides, oxides, and graphite in and around the ore bodies of Ducktown, Tennessee: Econ. Geology, v. 75, p. 1010-1021.

Newton, R. C., and Haselton, H. T., 1981, Thermodynamics of the garnet–plagioclase–Al_2SiO_5–quartz geobarometer, *in* Newton, R. C., Navrotsky, A., and Wood, B. J., eds., Thermodynamics of Minerals and Melts: New York, Springer-Verlag, p. 131-147.

Ohmoto, H., and Kerrick, D. M., 1977, Devolatilization equilibria in graphitic systems: Am. Jour. Sci., v. 277, p. 1013-1044.

Perchuk, L. L., Podlesskii, K. K., and Aranovich, L. Ya., 1981, Calculation of thermodynamic properties of end-member minerals from natural parageneses, *in* Newton, R. C., Navrotsky, A., and Wood, B. J., eds., Thermodynamics of Minerals and Melts: New York, Springer-Verlag, p. 111-129.

Popp, R. K., Gilbert, M. C., and Craig, J. R., 1977, Stability of Fe–Mg amphiboles with respect to sulfur fugacity: Am. Mineralogist, v. 62, p. 13-30.

Richardson, S. W., 1968, Staurolite stability in a part of the system Fe-Al-Si-O-H: Jour. Petrology, v. 9, p. 467-488.

Robie, R. A., Hemingway, B. S., and Fisher, J. R., 1978, Thermodynamic properties of minerals and related substances at 298.15°K and 1 bar (10^5 pascals) pressure and at higher temperatures: U.S. Geol. Survey Bull., no. 1452, 456 p.

Robinson, P., and Tracy, R. J., 1977, Sulfide–silicate–oxide equilibria in sillimanite–K-feldspar grade pelitic schists, central Massachusetts: EOS, v. 58, p. 524.

Rumble, D., 1978, Mineralogy, petrology, and oxygen isotopic geochemistry of the Clough Formation, Black Mountain, West New Hampshire, USA: Jour. Petrology, v. 19, p. 317-340.

Salotti, C. A., 1969, The metamorphic origin of the present Ducktown, Tennessee ore deposits: Econ. Geology, v. 64, p. 118.

Seifert, F., 1970, Low-temperature compatibility relations of cordierite in haplopelites of the system K_2O–MgO–Al_2O_3–SiO_2–H_2O: Jour. Petrology, v. 11, p. 73-99.

Thompson, A. B., Lyttle, P. T., and Thompson, J. B., Jr., 1977, Mineral reactions and A–Na–K and A–F–M facies types in the Gassetts schist, Vermont: Am. Jour. Sci., v. 277, p. 1124-1151.

Thompson, J. B., Jr., 1972, Oxides and sulfides in regional metamorphism of pelitic schists: Internat. Geol. Cong., 24th, Montreal 1972, sec. 10, p. 27-35.

Toulmin, P., III, and Barton, P. B., 1964, A thermodynamic study of pyrite and pyrrhotite: Geochim. et Cosmochim. Acta, v. 28, p. 641-671.

Tracy, R. J., 1978, High grade metamorphic reactions and partial melting in pelitic schist, west-central Massachusetts: Am. Jour. Sci., v. 278, p. 150-178.

Tso, J. L., Gilbert, M. C., and Craig, J. R., 1979, Sulfidation of synthetic biotites: Am. Mineralogist, v. 64, p. 304-316.

Vokes, F. M., 1969, A review of the metamorphism of sulfide deposits: Earth-Science Rev., v. 5, p. 99-143.

Wenk, E., 1962, Plagioklas als Indexmineral in den Zentralalpen: Schweiz. min. pet. Mitt., v. 42, p. 139-152.

Zen, E-An, and Albee, A. L., 1964, Co-existent muscovite and paragonite in pelitic schists: Am. Mineralogist, v. 49, p. 904-925.